Mueller Navelet jets at LHC:
A clean test of QCD resummation effects at high energy?

Bertrand Ducloué

Laboratoire de Physique Théorique d'Orsay

Grenoble, January 16th 2013

in collaboration with
L. Szymanowski (NCBJ, Warsaw), S. Wallon (UPMC & LPT Orsay)

D. Colferai; F. Schwennsen, L. Szymanowski, S. Wallon
JHEP 1012:026 (2010) 1-72 [arXiv:1002.1365 [hep-ph]]

B.D., L. Szymanowski, S. Wallon, in preparation [arXiv:1208.6111 [hep-ph]]

- One of the important longstanding theoretical questions raised by QCD is its behaviour in the perturbative Regge limit $s \gg -t$
- Based on theoretical grounds, one should identify and test suitable observables in order to test this peculiar dynamics

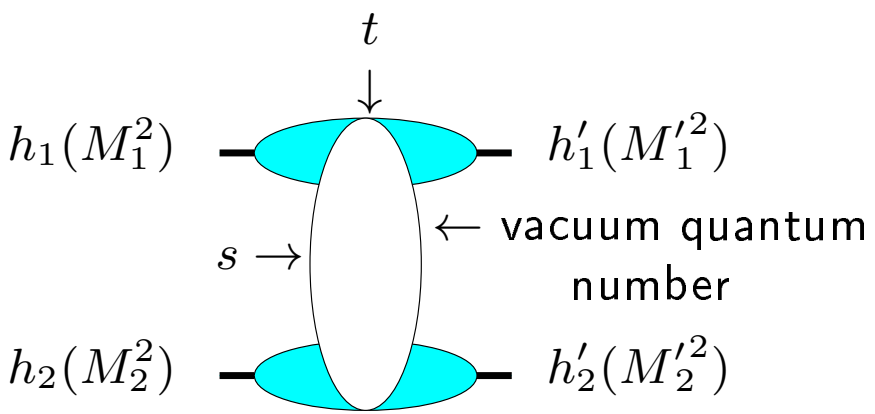

hard scales: $M_1^2,\ M_2^2 \gg \Lambda_{QCD}^2$ or $M_1'^2,\ M_2'^2 \gg \Lambda_{QCD}^2$ or $t \gg \Lambda_{QCD}^2$
where the $t-$channel exchanged state is the so-called hard Pomeron

The different regimes of QCD

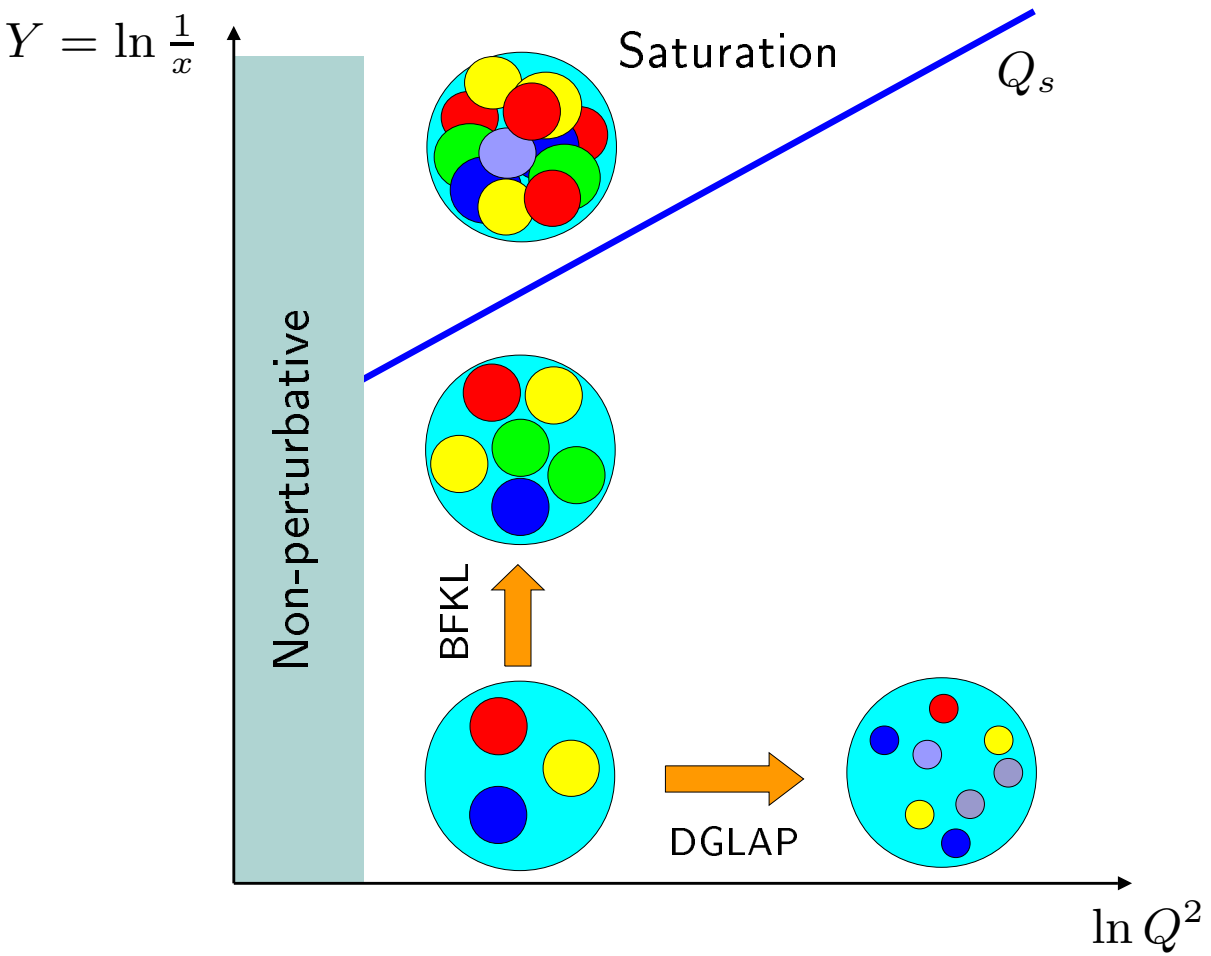

Resummation in QCD: DGLAP vs BFKL

Small values of α_S (perturbation theory applies due to hard scales) can be compensated by large logarithmic enhancements.
$\Rightarrow$ resummation of $\sum_n (\alpha_S \ln A)^n$ series

DGLAP	BFKL
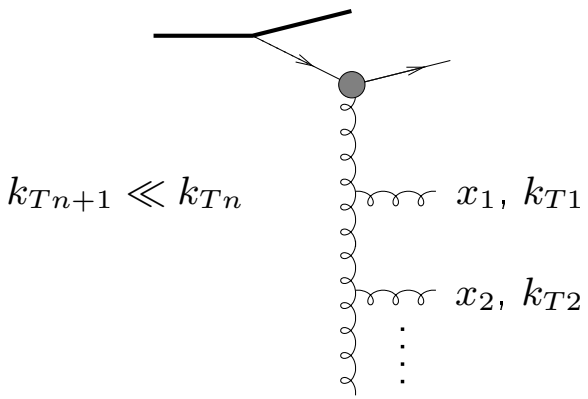	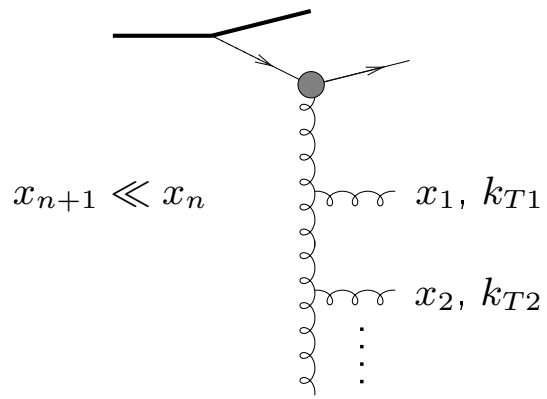
strong ordering in k_T	strong ordering in x
$\sum(\alpha_S \ln \frac{Q^2}{\mu^2})^n$	$\sum(\alpha_S \ln \frac{s}{s_0})^n$

When $\sqrt{s}$ becomes very large, it is expected that a BFKL description is needed to get accurate predictions

How to test QCD in the perturbative Regge limit?

What kind of observables?

- perturbation theory should be applicable:
  selecting external or internal probes with transverse sizes $\ll 1/\Lambda_{QCD}$ or by choosing large t in order to provide the hard scale

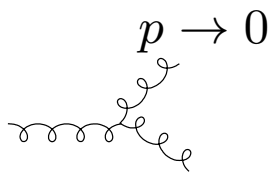

- governed by the *soft* perturbative dynamics of QCD

and *not* by its *collinear* dynamics

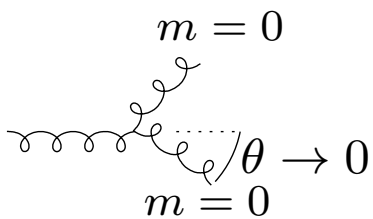

$\Rightarrow$ select semi-hard processes with $s \gg p_{T\,i}^2 \gg \Lambda_{QCD}^2$ where $p_{T\,i}^2$ are typical transverse scale, all of the same order

QCD in the perturbative Regge limit

The amplitude can be written as:

$\mathcal{A} =$ 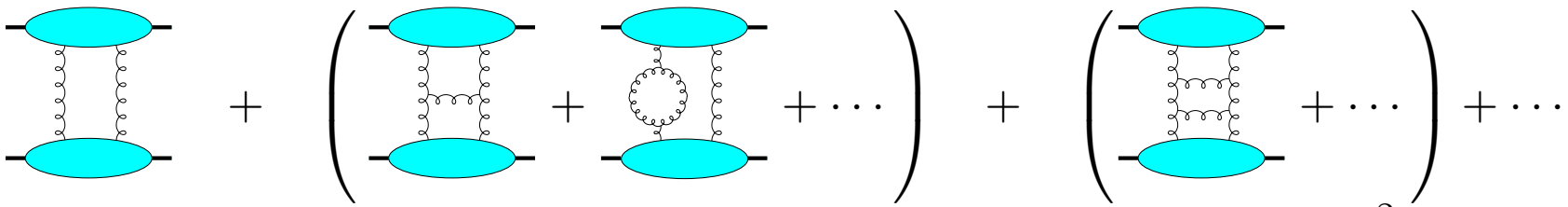 $+ \cdots$

$\sim s$ $\qquad$ $\sim s\,(\alpha_s \ln s)$ $\qquad$ $\sim s\,(\alpha_s \ln s)^2$

this can be put in the following form :

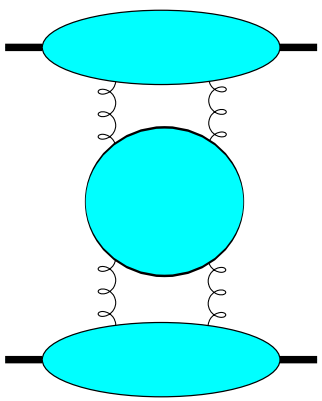

$\leftarrow$ Impact factor

$\leftarrow$ Green's function

$\leftarrow$ Impact factor

Higher order corrections

- Higher order corrections to BFKL kernel are known at NLL order (Lipatov Fadin; Camici, Ciafaloni), now for arbitrary impact parameter
  $\alpha_S \sum_n (\alpha_S \ln s)^n$ resummation

- impact factors are known in some cases at NLL
  - $\gamma^* \to \gamma^*$ at $t = 0$ (Bartels, Colferai, Gieseke, Kyrieleis, Qiao; Balitski, Chirilli)
  - forward jet production (Bartels, Colferai, Vacca)
  - inclusive production of a pair of hadrons separated by a large interval of rapidity (Ivanov, Papa)
  - $\gamma_L^* \to \rho_L$ in the forward limit (Ivanov, Kotsky, Papa)

Mueller-Navelet jets

- Consider two jets (hadrons flying within a narrow cone) separated by a large rapidity, i.e. each of them almost fly in the direction of the hadron "close" to it, and with very similar transverse momenta
- in a pure LO collinear treatment, these two jets should be emitted back to back at leading order: $\Delta\phi - \pi = 0$ ($\Delta\phi = \phi_1 - \phi_2 =$ relative azimuthal angle) and $k_{\perp 1}$=$k_{\perp 2}$. There is no phase space for (untagged) emission between them

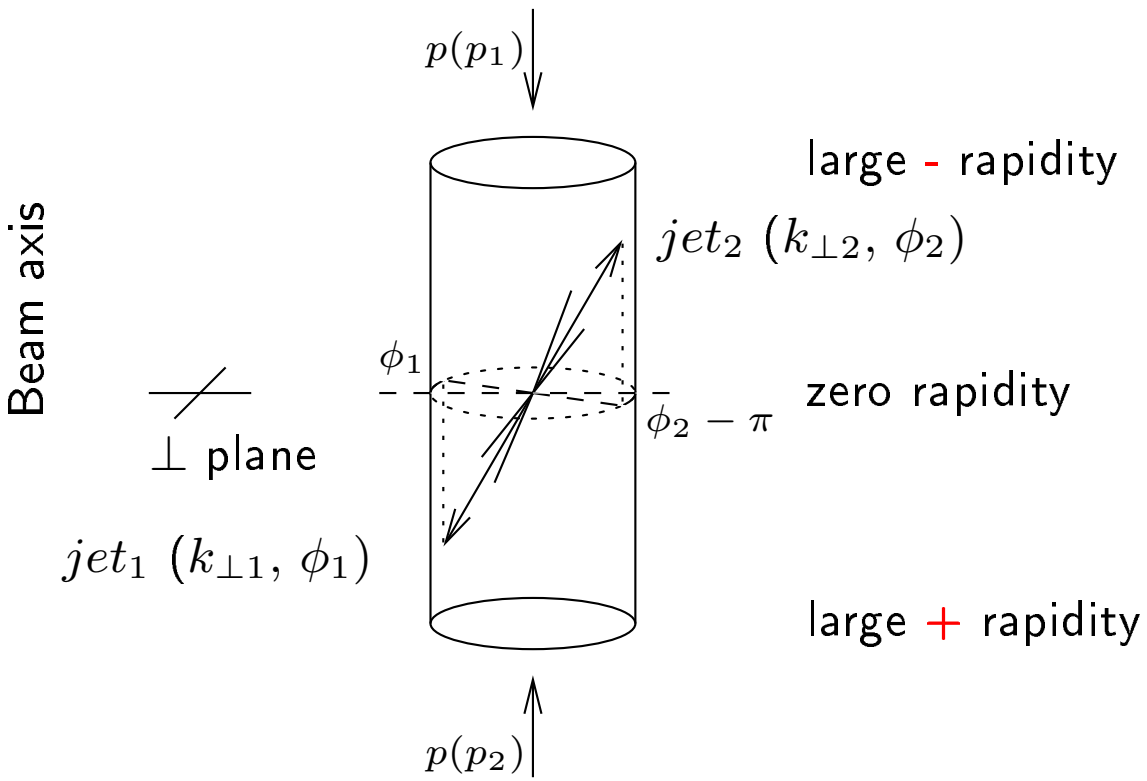

k_T-factorized differential cross-section

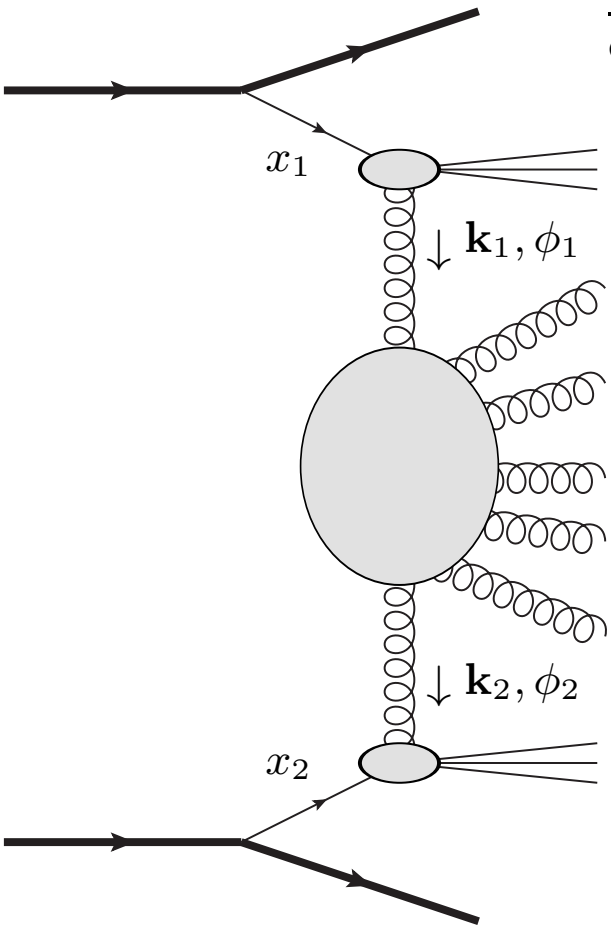

$$\frac{\mathrm{d}\sigma}{\mathrm{d}|\mathbf{k}_{J1}|\,\mathrm{d}|\mathbf{k}_{J2}|\,\mathrm{d}y_{J1}\,\mathrm{d}y_{J2}} = \int \mathrm{d}\phi_{J1}\,\mathrm{d}\phi_{J2} \int \mathrm{d}^2\mathbf{k}_1\,\mathrm{d}^2\mathbf{k}_2$$

$$\times \Phi(\mathbf{k}_{J1}, x_{J1}, -\mathbf{k}_1)$$

$$\times G(\mathbf{k}_1, \mathbf{k}_2, \hat{s})$$

$$\times \Phi(\mathbf{k}_{J2}, x_{J2}, \mathbf{k}_2)$$

with $\Phi(\mathbf{k}_{J2}, x_{J2}, \mathbf{k}_2) = \int \mathrm{d}x_2\, f(x_2) V(\mathbf{k}_2, x_2)$ $\quad f \equiv$ PDF $\quad x_J = \frac{|\mathbf{k}_J|}{\sqrt{s}} e^{y_J}$

- in LL BFKL ($\sim \sum (\alpha_s \ln s)^n$), the emission between these jets leads to a strong decorrelation between the jets, incompatible with $p\bar{p}$ Tevatron collider data

- up to recently, the subseries $\alpha_s \sum (\alpha_s \ln s)^n$ NLL was included only in the Green's function, and not inside the jet vertices
  Sabio Vera, Schwennsen
  Marquet, Royon

- the importance of these corrections was not known

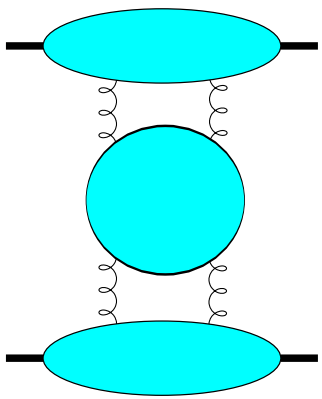

Results for an asymmetric configuration

In this section we choose the cuts as

- $35\,\mathrm{GeV} < |\mathbf{k}_{J1}| < 60\,\mathrm{GeV}$
- $50\,\mathrm{GeV} < |\mathbf{k}_{J2}| < 60\,\mathrm{GeV}$
- $0 < y_1\,, y_2 < 4.7$

Such an asymmetric configuration is required by DGLAP like approaches, which are unstable for symmetric configurations.

Results: asymmetric configuration

Cross-section: NLO DGLAP versus NLL BFKL

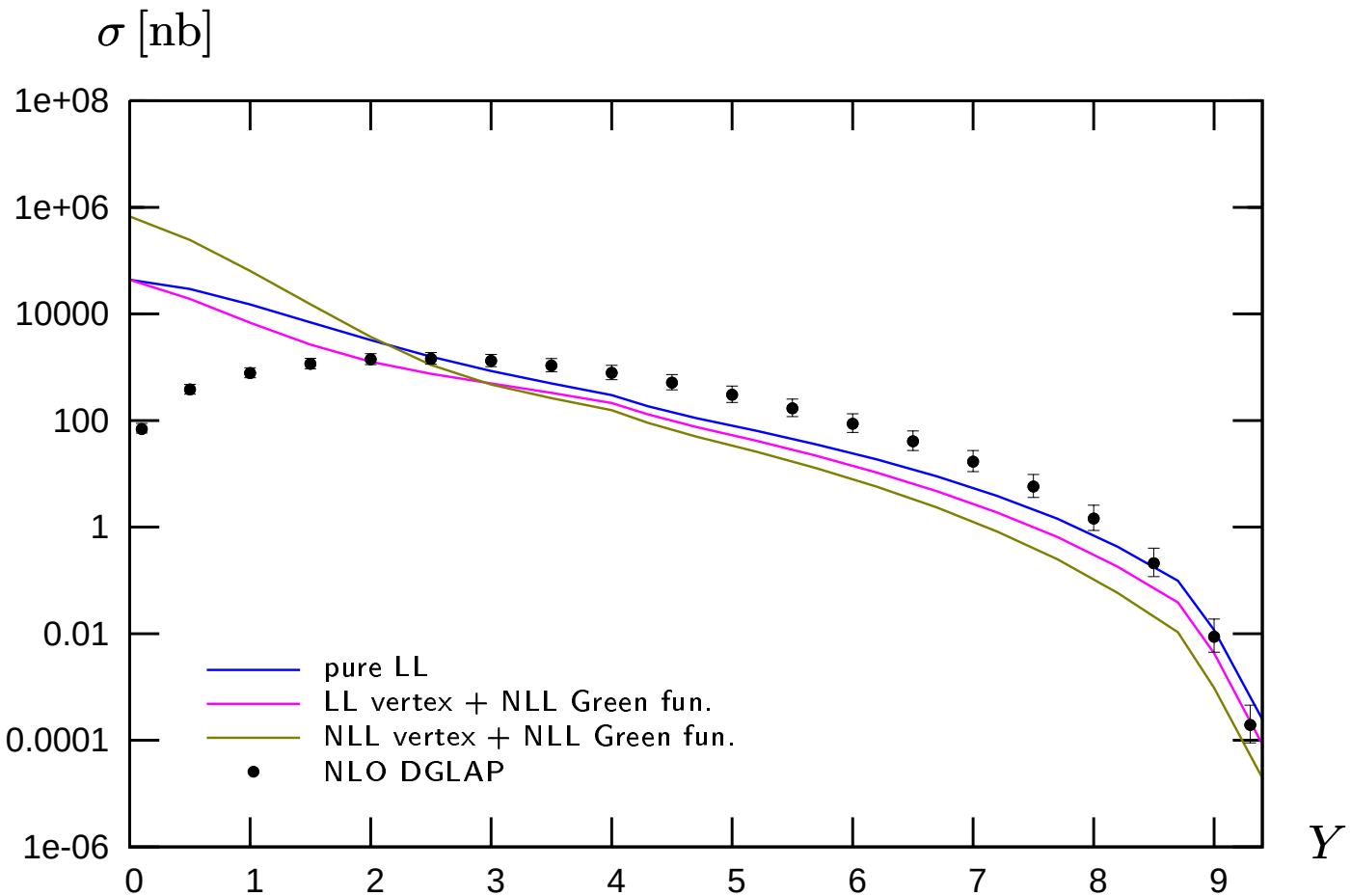

$35\,\mathrm{GeV} < |\mathbf{k}_{J1}| < 60\,\mathrm{GeV}$

$50\,\mathrm{GeV} < |\mathbf{k}_{J2}| < 60\,\mathrm{GeV}$

$0 < y_1 < 4.7$

$0 < y_2 < 4.7$

dots = based on the NLO DGLAP parton generator *Dijet* (thanks to M. Fontannaz)

Results: asymmetric configuration

Cross-section: stability with respect to s_0 and $\mu_R = \mu_F$ changes

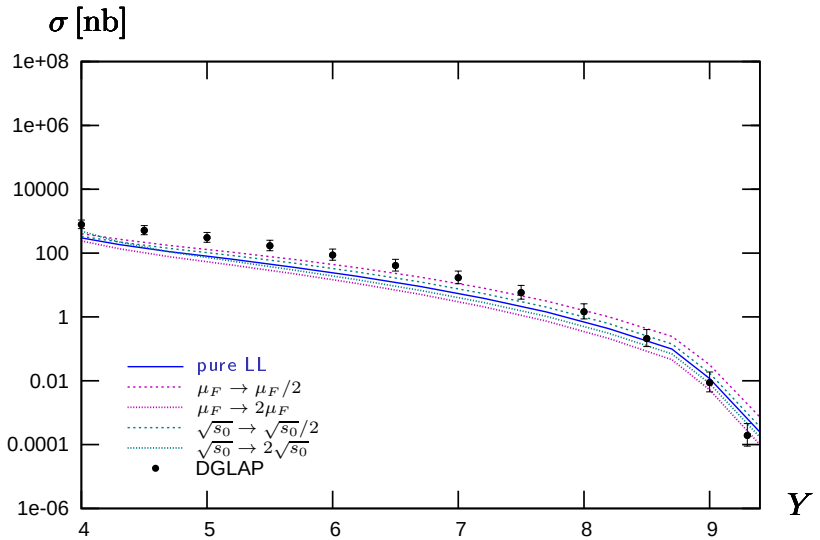

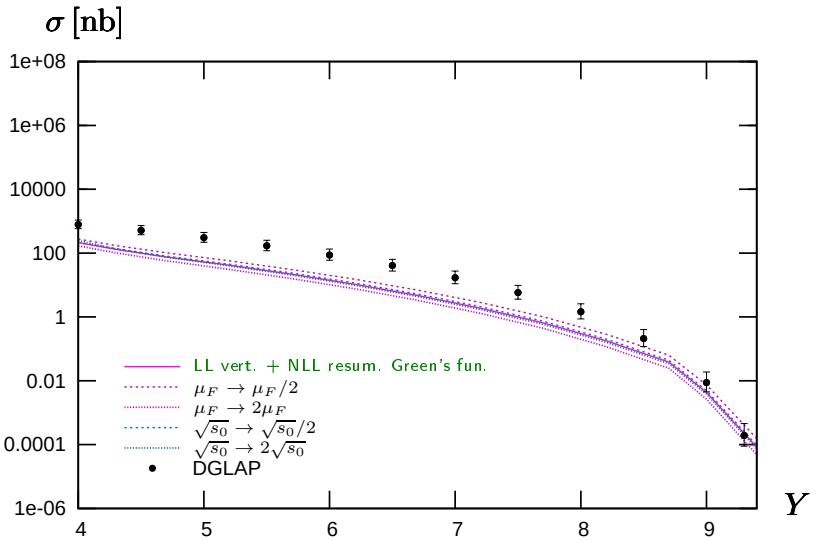

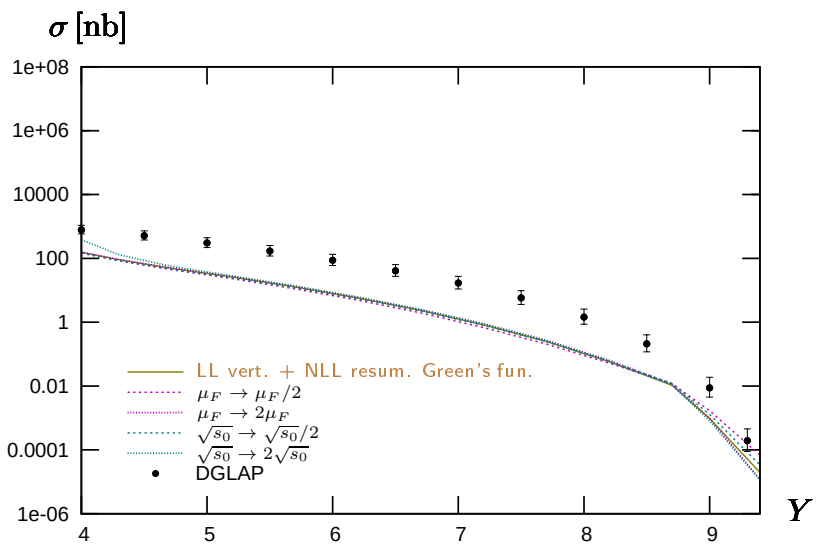

Results: asymmetric configuration

Compared cross-sections including uncertainties

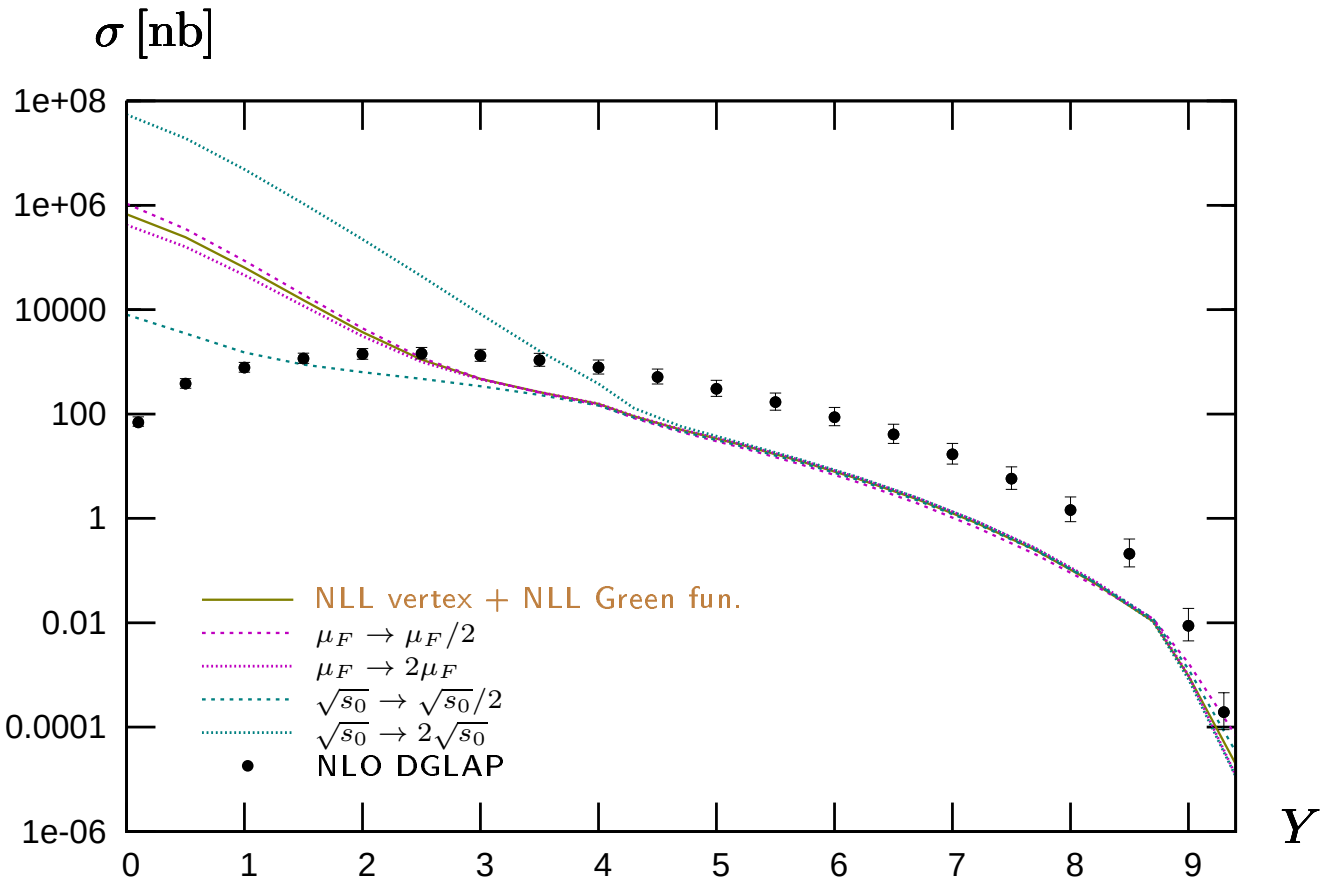

$35\,\mathrm{GeV} < |\mathbf{k}_{J1}| < 60\,\mathrm{GeV}$

$50\,\mathrm{GeV} < |\mathbf{k}_{J2}| < 60\,\mathrm{GeV}$

$0 < y_1 < 4.7$

$0 < y_2 < 4.7$

- Putting (almost) the same scale, exactly the same cuts, we get a noticeable difference between NLO DGLAP and NLL BFKL for $4.5 < Y < 8.5$: $\sigma_{\mathrm{NLO}} > \sigma_{\mathrm{NLL\,BFKL}}$
- This result is rather stable w.r.t s_0 and μ choices.

Azimuthal correlation $\langle \cos\varphi \rangle$: NLO DGLAP versus NLL BFKL

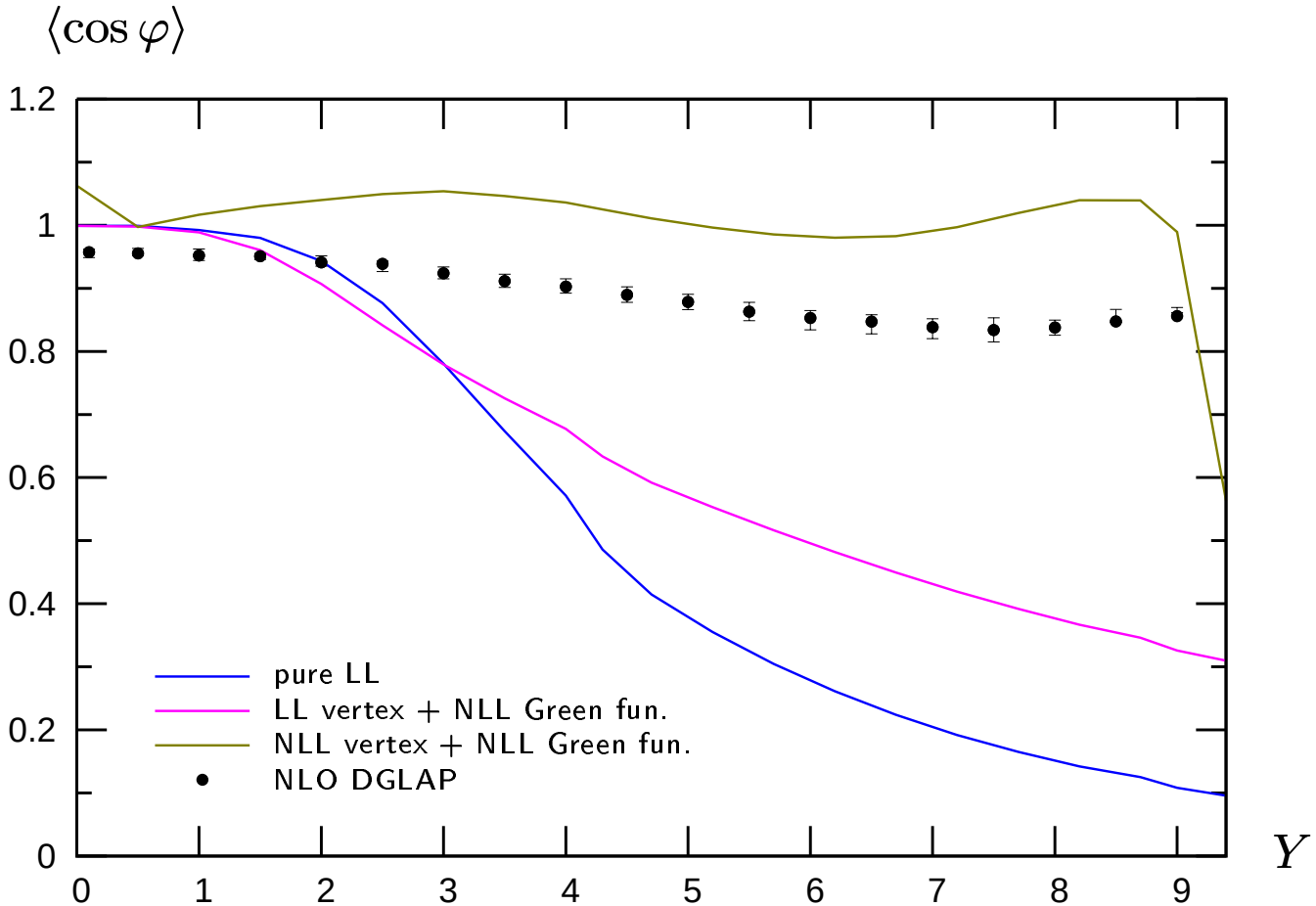

$35\,\mathrm{GeV} < |\mathbf{k}_{J1}| < 60\,\mathrm{GeV}$

$50\,\mathrm{GeV} < |\mathbf{k}_{J2}| < 60\,\mathrm{GeV}$

$0 < y_1 < 4.7$

$0 < y_2 < 4.7$

dots = based on the NLO DGLAP parton generator *Dijet* (thanks to M. Fontannaz)

Azimuthal correlation: $\langle \cos\varphi \rangle$

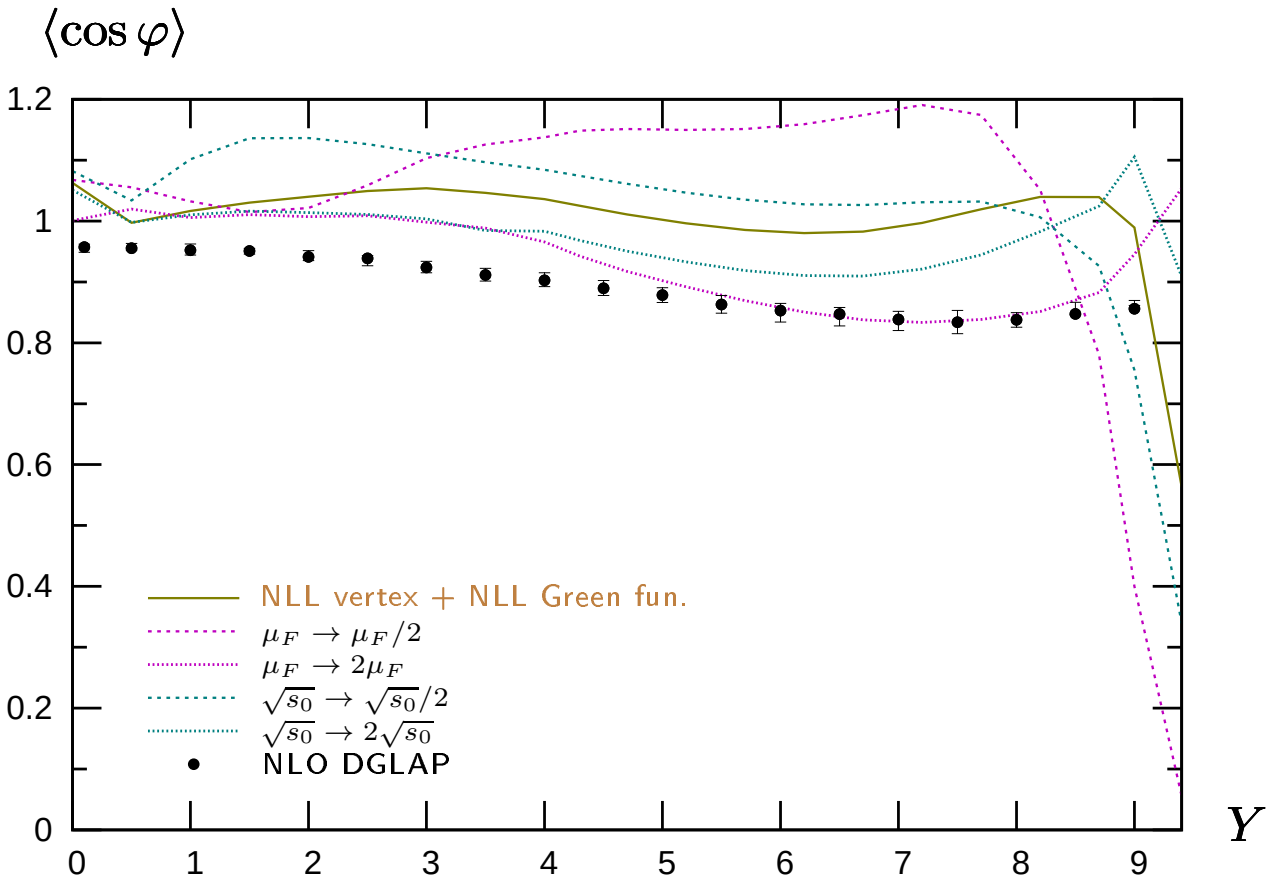

$35\,\mathrm{GeV} < |\mathbf{k}_{J1}| < 60\,\mathrm{GeV}$

$50\,\mathrm{GeV} < |\mathbf{k}_{J2}| < 60\,\mathrm{GeV}$

$0 < y_1 < 4.7$

$0 < y_2 < 4.7$

- Putting (almost) the same scale, exactly the same cuts, we get a difference between NLO DGLAP and NLL BFKL for $4.5 < Y < 8.5$
- This difference is washed-out because of s_0 and μ dependency: $\langle \cos\varphi \rangle_{\mathrm{NLO}} \sim \langle \cos\varphi \rangle_{\mathrm{NLL\,BFKL}}$

Azimuthal correlation $\langle\cos 2\varphi\rangle/\langle\cos\varphi\rangle$: NLO versus NLL BFKL

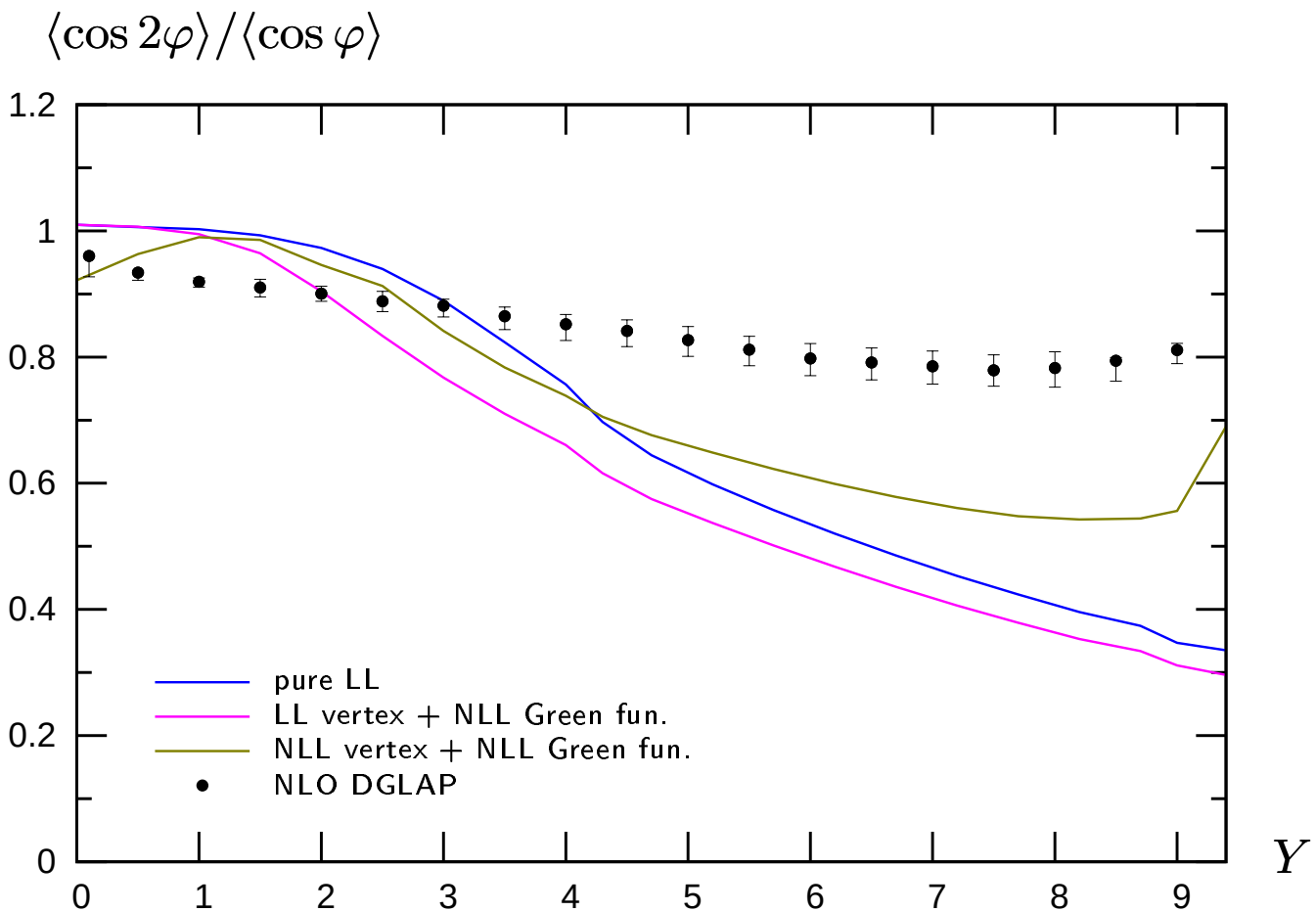

$35\,\mathrm{GeV} < |\mathbf{k}_{J1}| < 60\,\mathrm{GeV}$

$50\,\mathrm{GeV} < |\mathbf{k}_{J2}| < 60\,\mathrm{GeV}$

$0 < y_1 < 4.7$

$0 < y_2 < 4.7$

dots = based on the NLO DGLAP parton generator *Dijet* (thanks to M. Fontannaz)

Results: asymmetric configuration

Azimuthal correlation: $\langle \cos 2\varphi \rangle / \langle \cos \varphi \rangle$

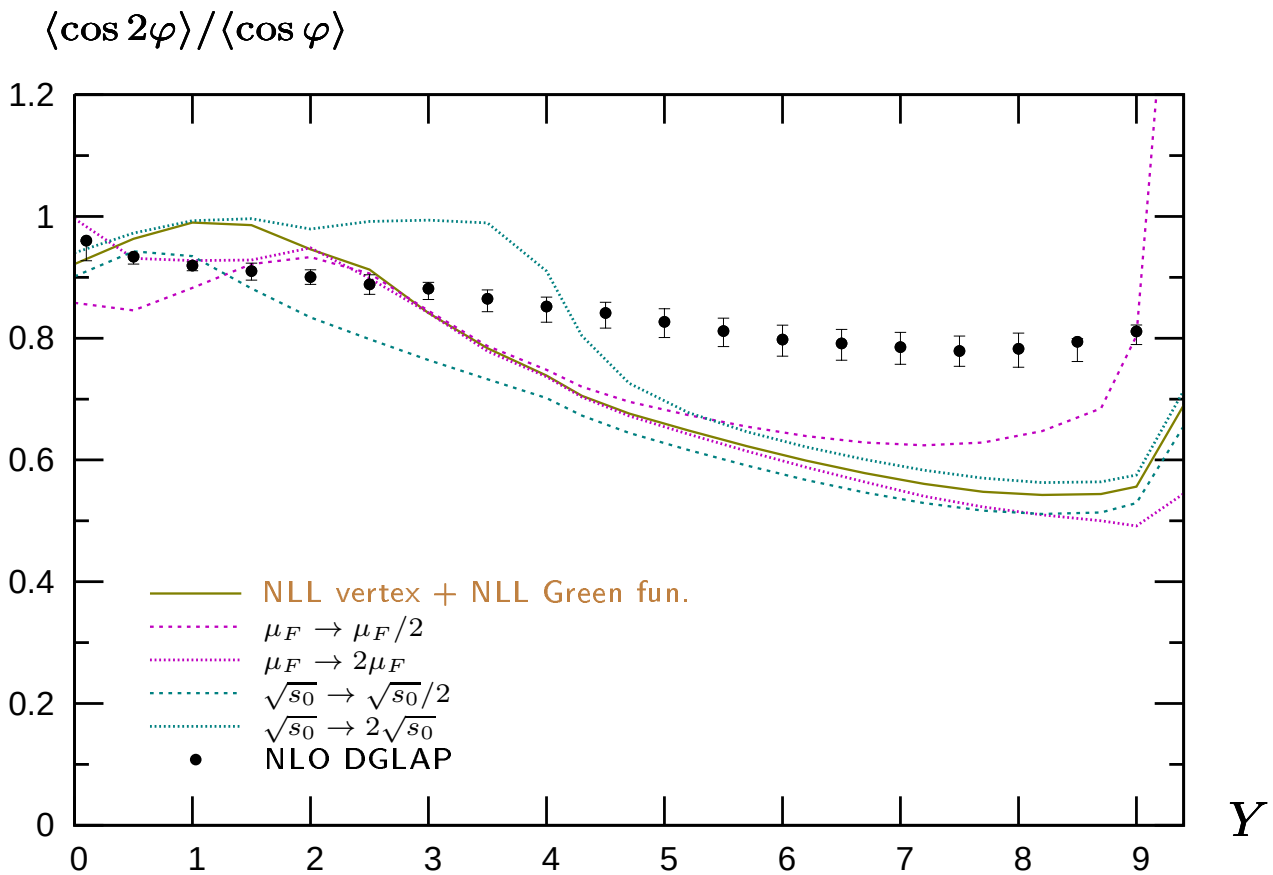

$$35\,\text{GeV} < |\mathbf{k}_{J1}| < 60\,\text{GeV}$$
$$50\,\text{GeV} < |\mathbf{k}_{J2}| < 60\,\text{GeV}$$

$$0 < y_1 < 4.7$$
$$0 < y_2 < 4.7$$

- NLO DGLAP and NLL BFKL differ for $4.5 < Y < 8$

$$\frac{\langle \cos 2\varphi \rangle_{\text{NLO}}}{\langle \cos \varphi \rangle_{\text{NLO}}} > \frac{\langle \cos 2\varphi \rangle_{\text{NLL BFKL}}}{\langle \cos \varphi \rangle_{\text{NLL BFKL}}}$$

- This result is rather stable w.r.t s_0 and μ choices.

Results for a symmetric configuration

In this section we show results for

- $35\,\mathrm{GeV} < |\mathbf{k}_{J1}|\,, |\mathbf{k}_{J2}| < 60\,\mathrm{GeV}$
- $0 < y_1\,, y_2 < 4.7$

These cuts should be close to the ones that will be used in forthcoming analyses by ATLAS or CMS.

note:

- results for $\langle \cos(n\phi) \rangle$ are similar to the asymmetric configuration
- the cross section is even larger

Azimuthal distribution

Computing $\langle \cos(n\phi) \rangle$ up to large values of n gives access to the angular distribution

$$\frac{1}{\sigma}\frac{d\sigma}{d\phi} = \frac{1}{2\pi}\left\{1 + 2\sum_{n=1}^{\infty} \cos\left(n\phi\right) \langle \cos\left(n\phi\right) \rangle \right\}$$

This is a quantity accessible at experiments like ATLAS and CMS

Results: symmetric configuration

Azimuthal distribution

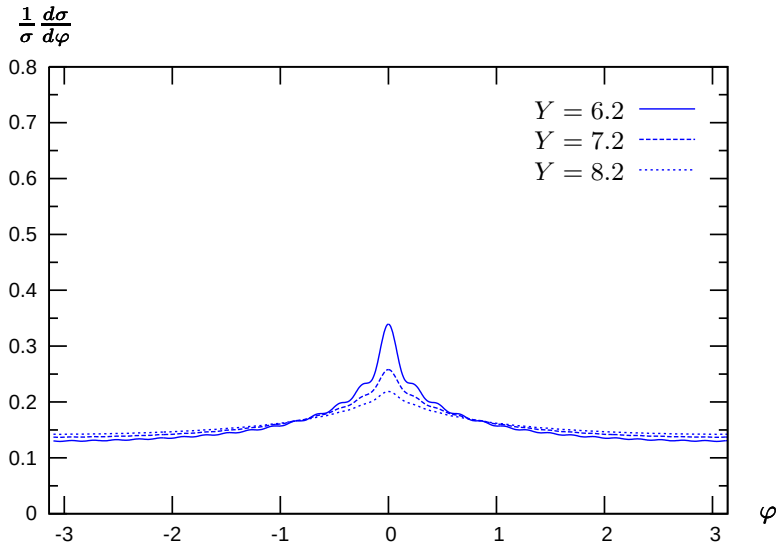

pure LL

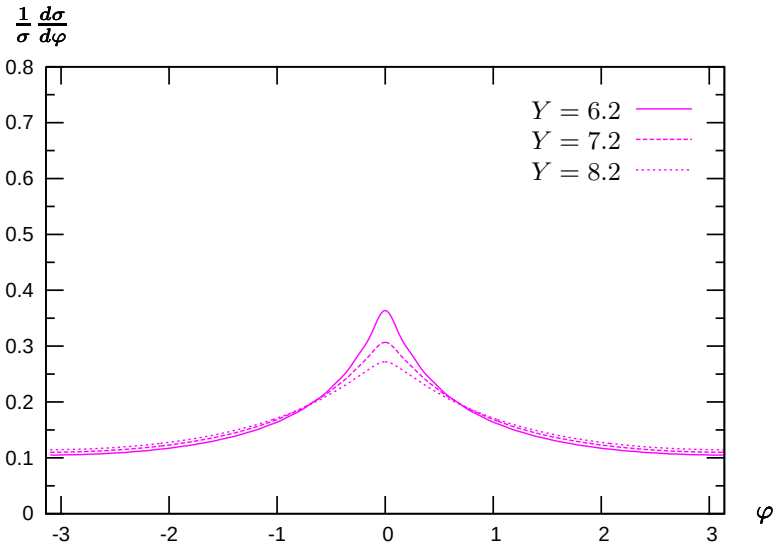

LL vertices + NLL Green's fun.

$$35\,\mathrm{GeV} < |\mathbf{k}_{J1}| < 60\,\mathrm{GeV}$$
$$35\,\mathrm{GeV} < |\mathbf{k}_{J2}| < 60\,\mathrm{GeV}$$

$$0 < y_1 < 4.7$$
$$0 < y_2 < 4.7$$

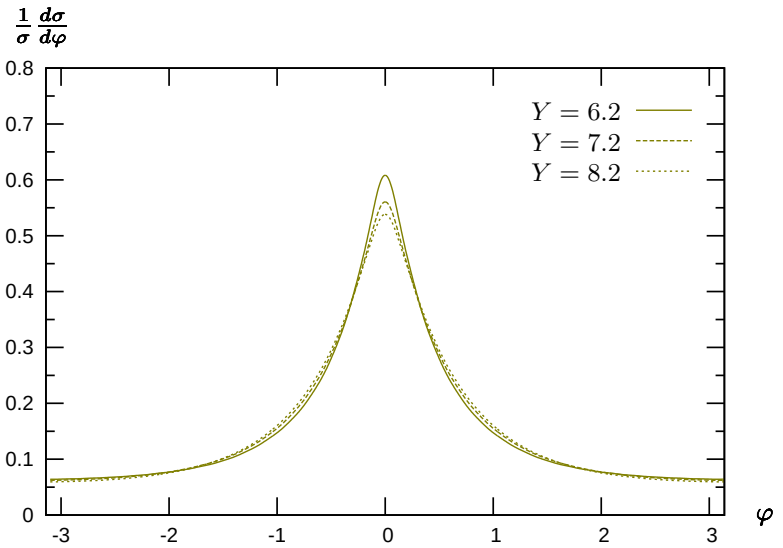

NLL vert. + NLL Green's fun.

Results: symmetric configuration

Azimuthal distribution: stability with respect to s_0 and $\mu_R = \mu_F$

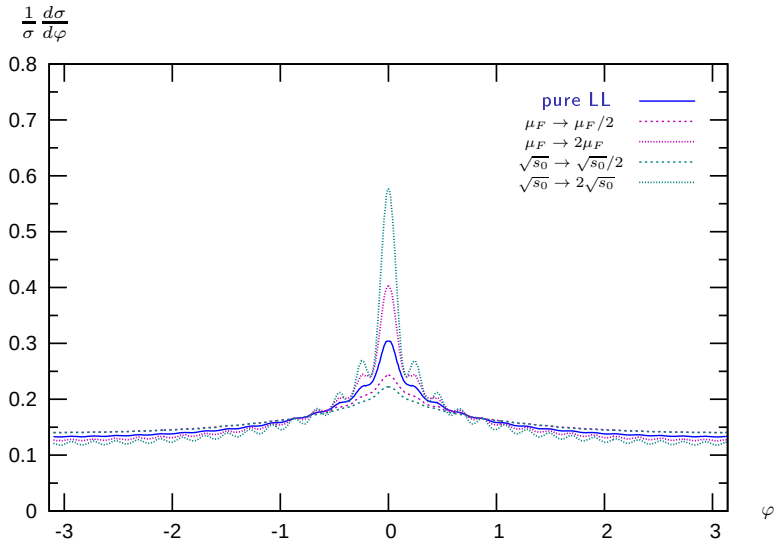

pure LL

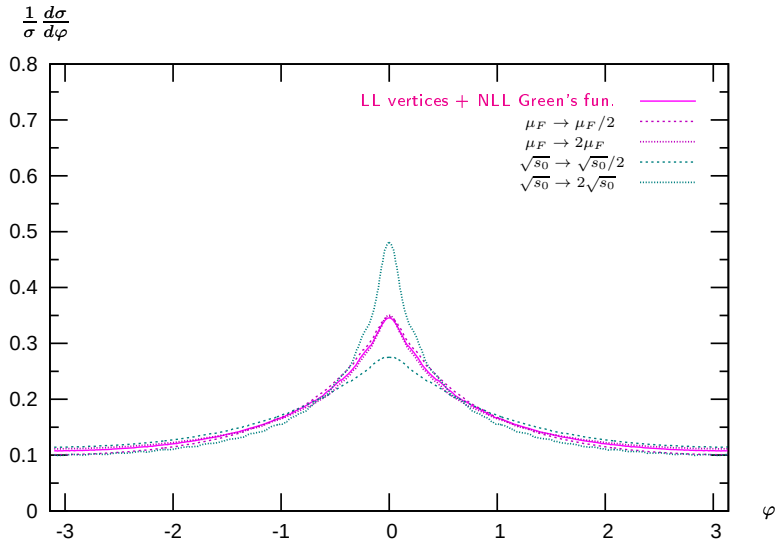

LL vertices + NLL Green's fun.

$35\,\text{GeV} < |\mathbf{k}_{J1}| < 60\,\text{GeV}$
$35\,\text{GeV} < |\mathbf{k}_{J2}| < 60\,\text{GeV}$

$0 < y_1 < 4.7$
$0 < y_2 < 4.7$

integrating on the bin:
$6 < Y = y_1 + y_2 < 9.4$

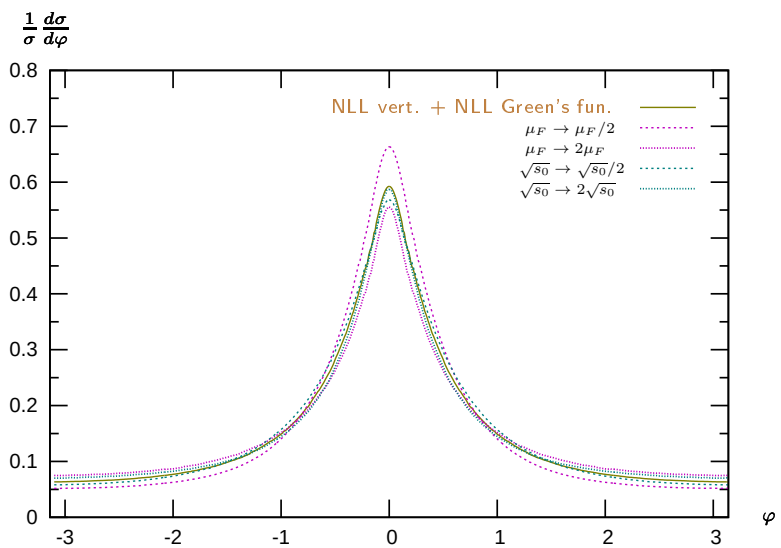

NLL vert. + NLL Green's fun.

Conclusion

- We have deepened our complete NLL analysis of Mueller-Navelet jets
- The effect of NLL corrections to the vertices is dramatic, similar to the NLL Green function corrections
- For the cross-section:
  makes prediction more stable with respect to variation of scales μ and s_0
  sizeably below NLO DGLAP
- Surprisingly small decorrelation effect
  $\langle \cos \varphi \rangle$ very flat in rapidity Y
  close to NLO DGLAP when taking into account the scale dependency
- For $\langle \cos 2\varphi \rangle / \langle \cos \varphi \rangle$ we see a difference between NLL BFKL and NLO DGLAP
- The φ distribution is strongly peaked around 0 and varies slowly with Y
- Mueller Navelet jets provide much more complicate observables than expected

Backup

Results: symmetric configuration

Azimuthal correlation

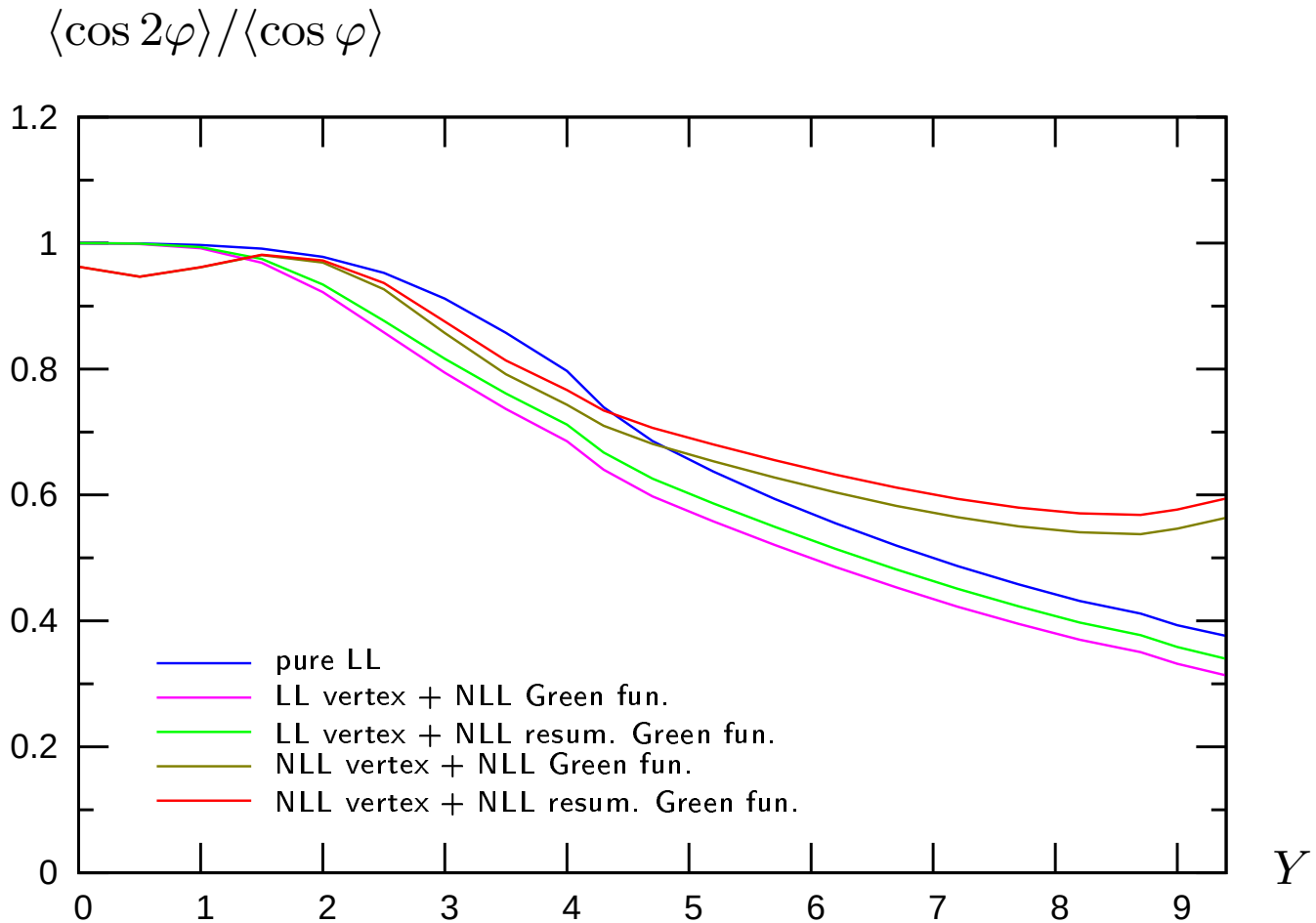

$35\,\mathrm{GeV} < |\mathbf{k}_{J1}| < 60\,\mathrm{GeV}$

$35\,\mathrm{GeV} < |\mathbf{k}_{J2}| < 60\,\mathrm{GeV}$

$0 < y_1 < 4.7$

$0 < y_2 < 4.7$

Results: symmetric configuration

Azimuthal correlation: stability with respect to s_0 and $\mu_R = \mu_F$

(here only the full NLL approach is shown)

$\langle \cos 2\varphi \rangle / \langle \cos \varphi \rangle$

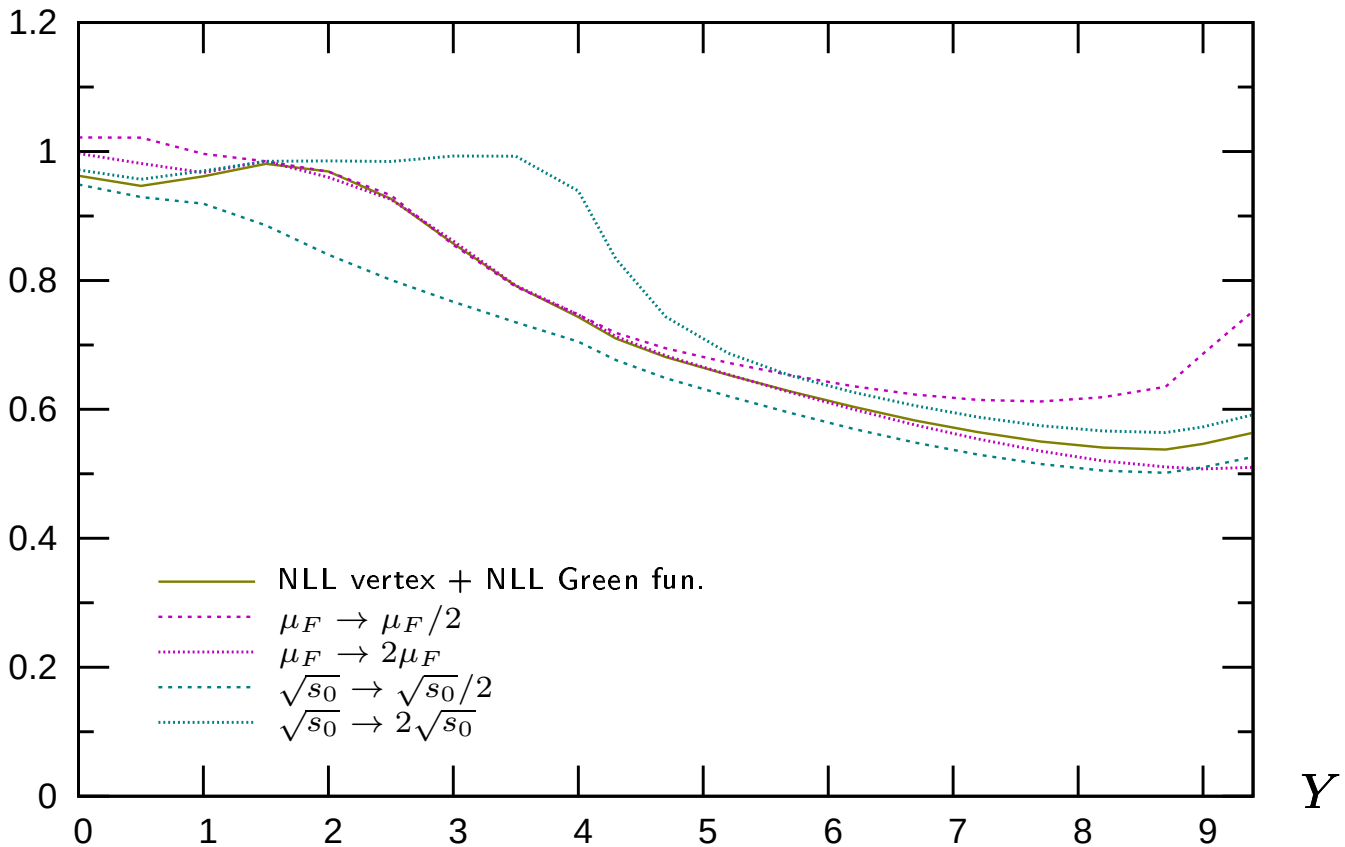

$35\,\mathrm{GeV} < |\mathbf{k}_{J1}| < 60\,\mathrm{GeV}$

$35\,\mathrm{GeV} < |\mathbf{k}_{J2}| < 60\,\mathrm{GeV}$

$0 < y_1 < 4.7$

$0 < y_2 < 4.7$

Very good stability in the range $5 < Y < 8$

Azimuthal correlation $\langle \cos\varphi \rangle$: PDF errors

Relative variation of $\langle \cos\varphi \rangle$ when using other PDF sets than MSTW 2008 (full NLL approach)

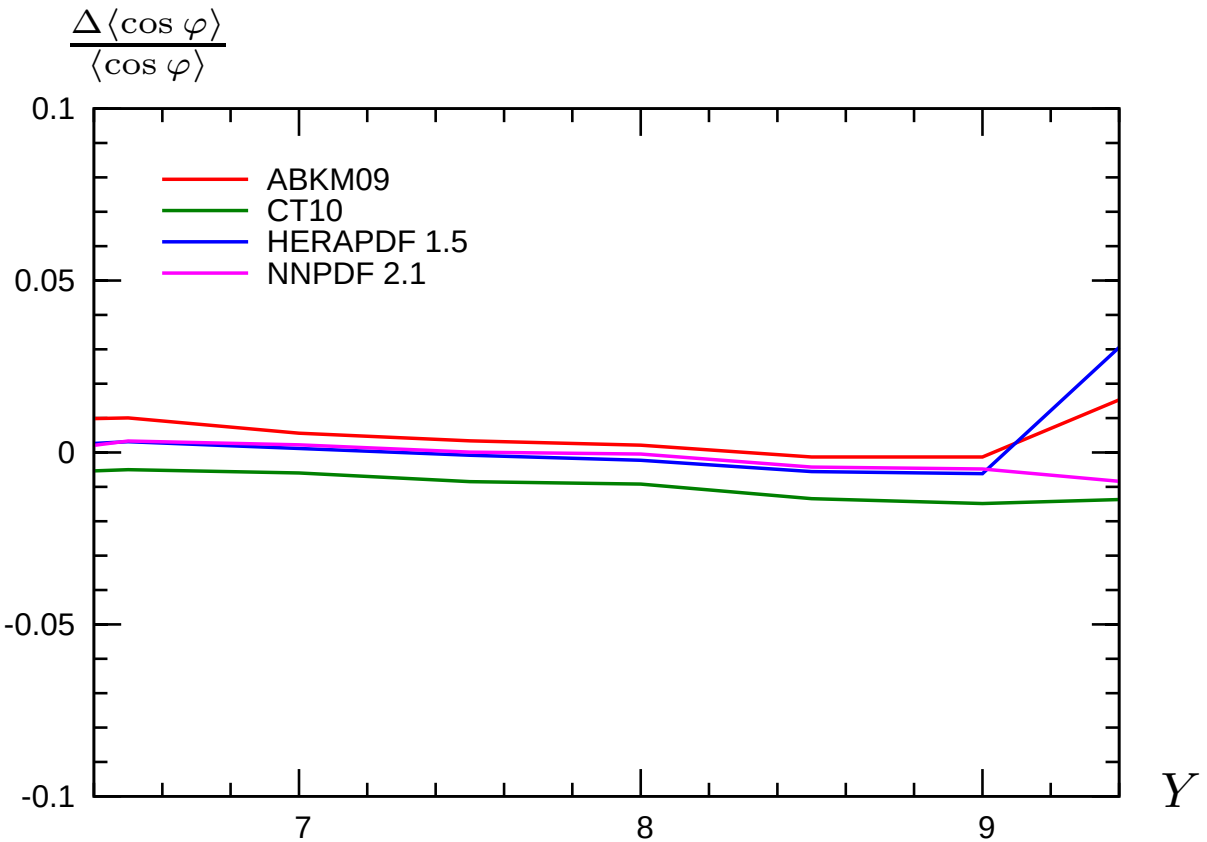

$|\mathbf{k}_{J1}| = |\mathbf{k}_{J2}| = 35\,\mathrm{GeV}$

$0 < y_1 < 4.7$

$0 < y_2 < 4.7$

$\langle \cos\varphi \rangle$ is much less sensitive to the PDFs than the cross section

(at LL $\langle \cos\varphi \rangle$ does not depend on the PDFs at all)

Azimuthal correlation: PDF errors

Relative variation of $\frac{\langle \cos 2\phi \rangle}{\langle \cos \phi \rangle}$ when using other PDF sets than MSTW 2008 (full NLL approach)

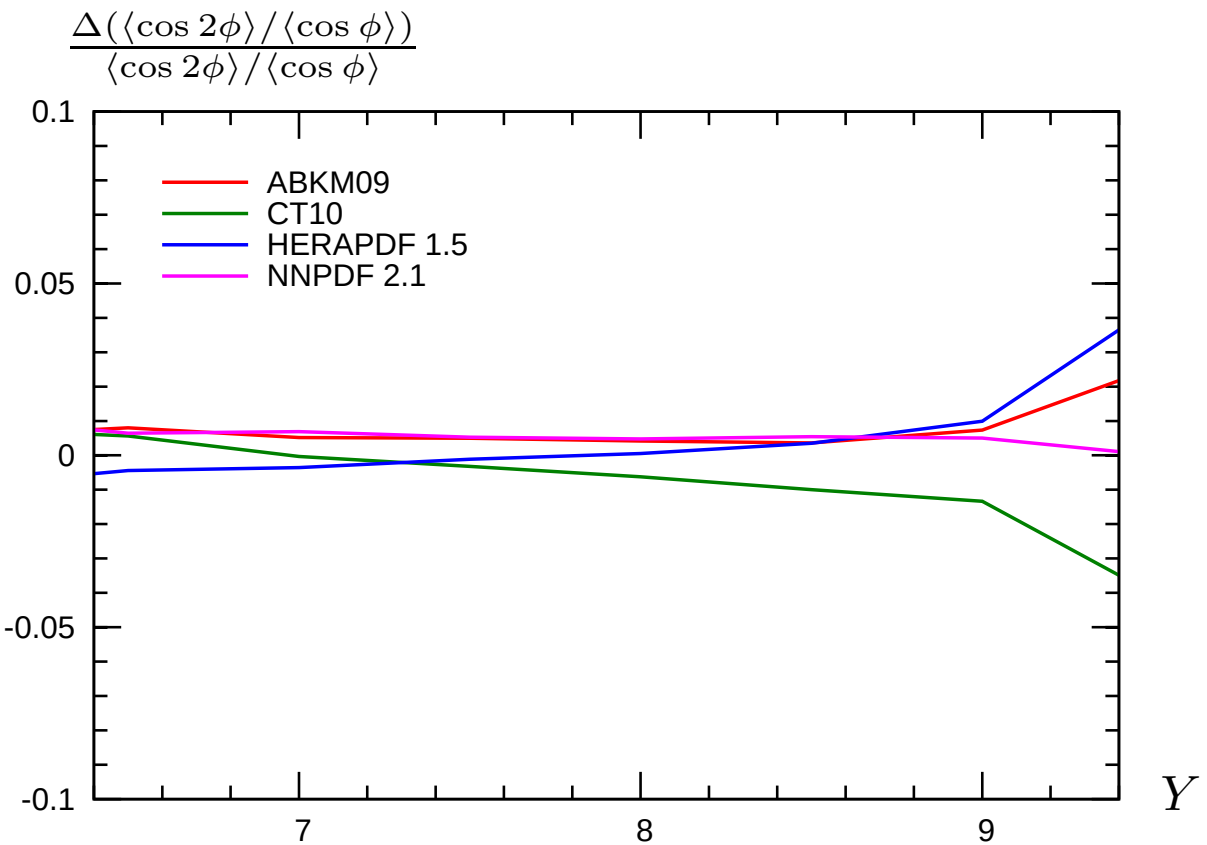

$|\mathbf{k}_{J1}| = |\mathbf{k}_{J2}| = 35\,\mathrm{GeV}$

$0 < y_1 < 4.7$

$0 < y_2 < 4.7$

$\langle \cos 2\varphi \rangle / \langle \cos \varphi \rangle$ is much less sensitive to the PDFs than the cross section

Comparison with NLO DGLAP for $\sqrt{s} = 14$ TeV

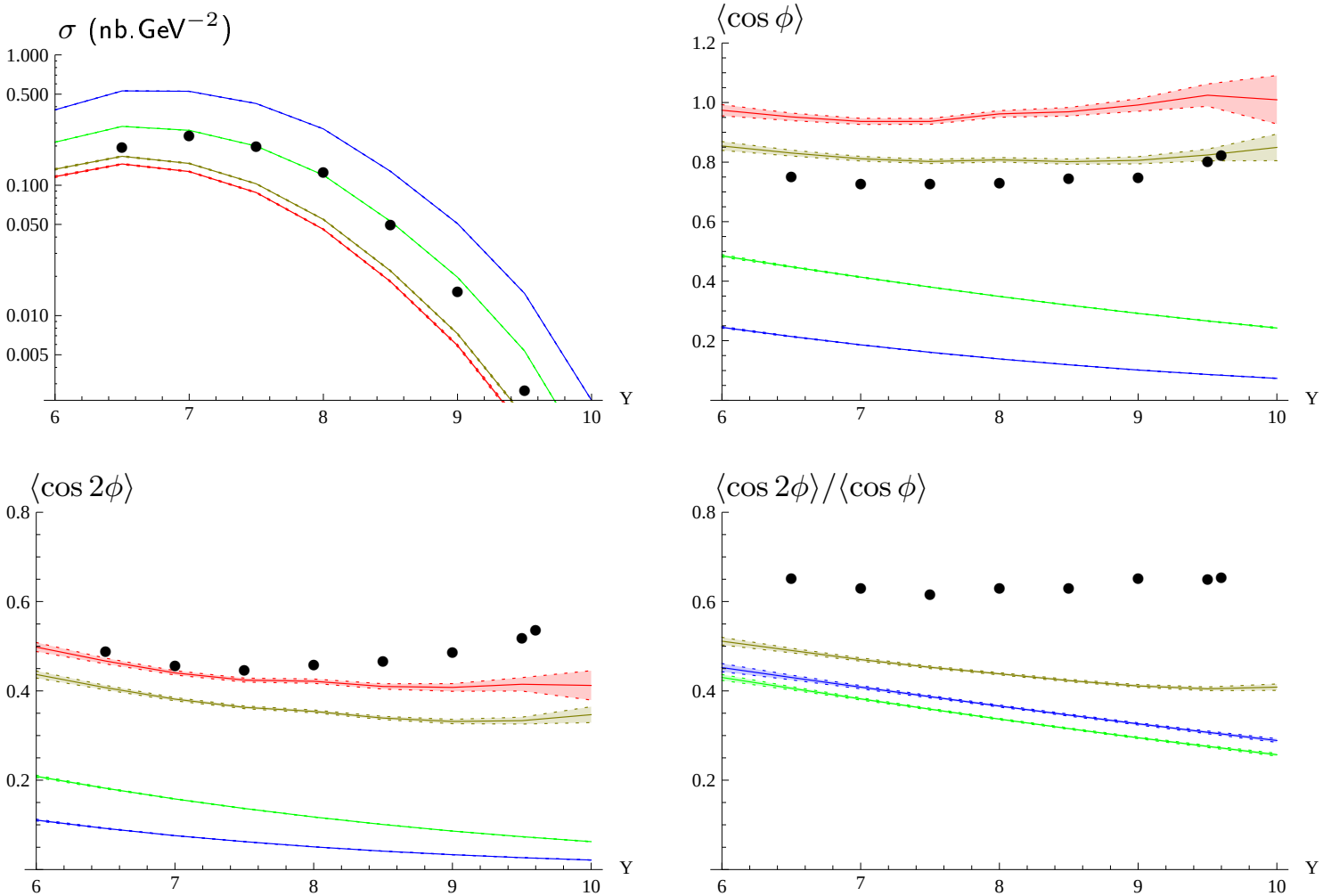

dots: based on the NLO DGLAP parton generator Dijet (thanks to M. Fontannaz)

Comparison in the simplified NLL Green's function + LL jet vertices scenario

- The integration $\int_{k_{J\,min}}^{\infty} dk_J$ can be performed analytically
- A comparison with the numerical integration based on code provides a good test of stability, valid for large Y

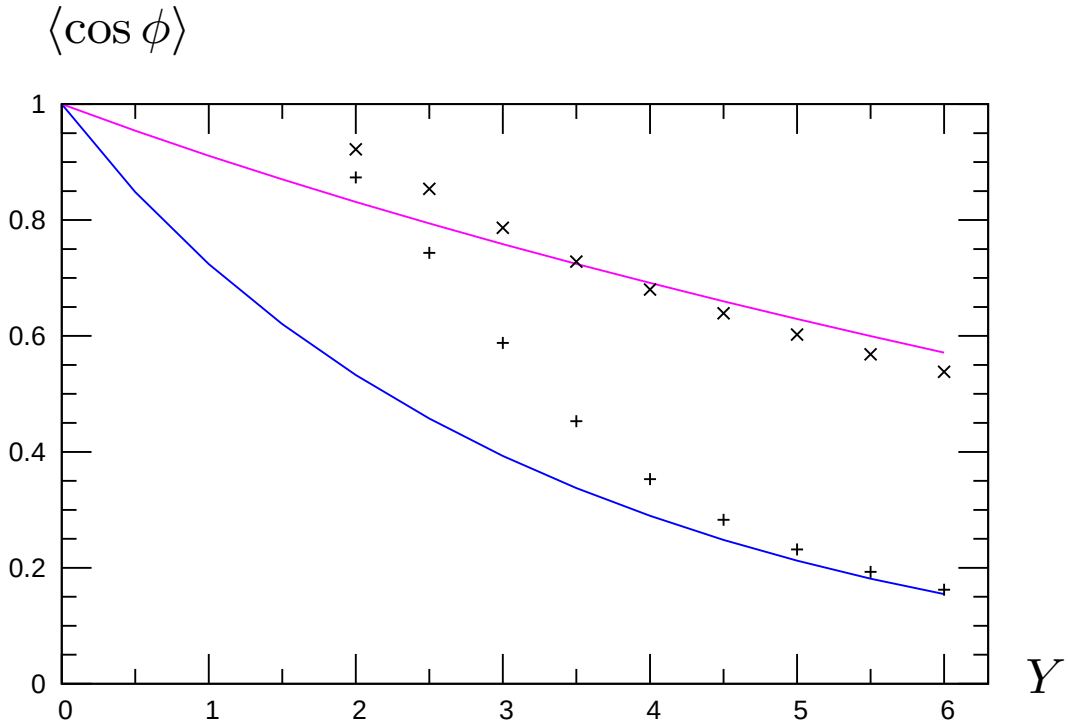

blue: LL

magenta: NLL Green's function + LL jet vertices scenario Sabio Vera, Schwennsen

×: numerical dk_J integration $k_{J1} > 20$ GeV and $k_{J2} > 50$ GeV

QCD in the perturbative Regge limit

- Small values of α_S (perturbation theory applies due to hard scales) can be compensated by large $\ln s$ enhancements. $\Rightarrow$ resummation of $\sum_n (\alpha_S \ln s)^n$ series (Balitski, Fadin, Kuraev, Lipatov)

$\mathcal{A} =$ 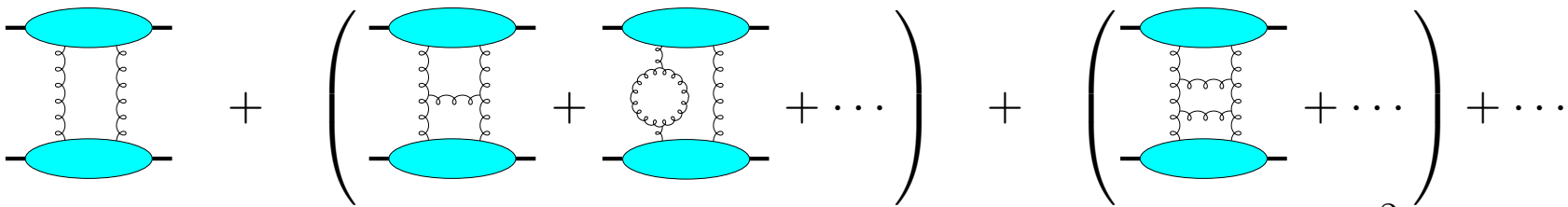 $+ \cdots$

$\sim s$ $\qquad$ $\sim s\,(\alpha_s \ln s)$ $\qquad$ $\sim s\,(\alpha_s \ln s)^2$

- this results in the effective BFKL ladder

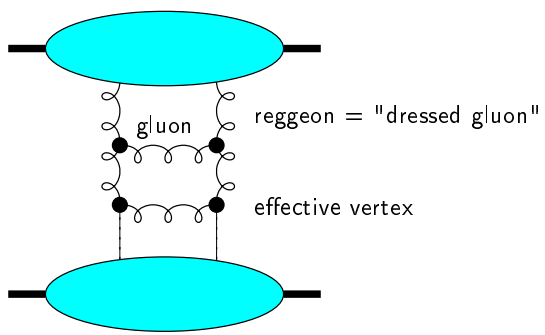

$$\Longrightarrow \sigma_{tot}^{h_1 h_2 \to anything} = \frac{1}{s} Im\mathcal{A} \sim s^{\alpha_{\mathbb{P}}(0)-1}$$

with $\alpha_{\mathbb{P}}(0) - 1 = C\,\alpha_s \quad (C > 0)$ Leading Log $\mathbb{P}$omeron
Balitsky, Fadin, Kuraev, Lipatov

Opening the boxes: Impact representation $\gamma^*\,\gamma^* \to \gamma^*\,\gamma^*$ as an example

- Sudakov decomposition: $k_i = \alpha_i\, p_1 + \beta_i\, p_2 + k_{\perp i}$ $\quad (p_1^2 = p_2^2 = 0,\ 2p_1 \cdot p_2 = s)$
- write $\qquad d^4k_i = \frac{s}{2}\, d\alpha_i\, d\beta_i\, d^2k_{\perp i} \qquad \left(\underline{k} = \text{Eucl.} \leftrightarrow k_\perp = \text{Mink.}\right)$
- $t-$channel gluons have non-sense polarizations at large s: $\epsilon_{NS}^{up/down} = \frac{2}{s}\, p_{2/1}$

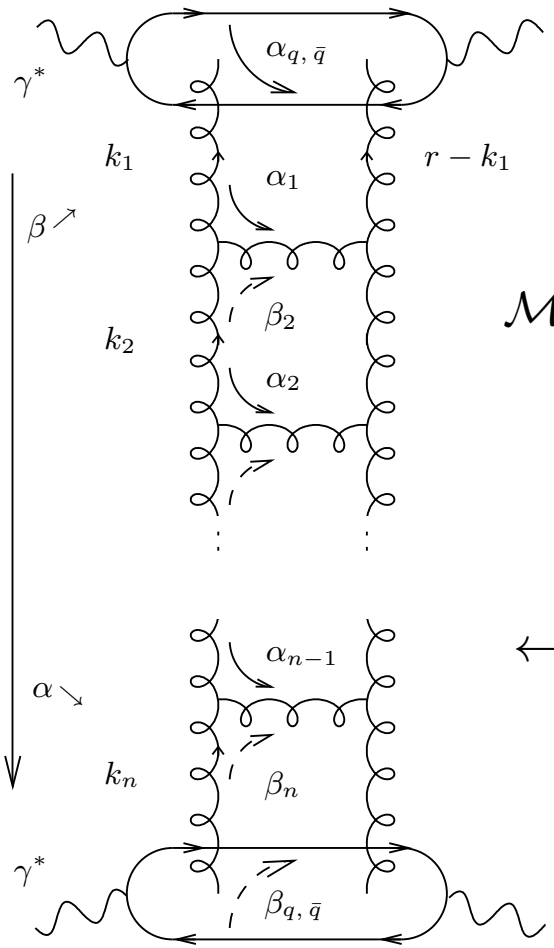

$\Rightarrow$ set $\alpha_1 = 0$ and $\int d\beta_1$ $\Rightarrow$ $\Phi^{\gamma^*\to\gamma^*}(\underline{k}_1, \underline{r} - \underline{k}_1)$
impact factor

$$\mathcal{M} = \frac{is}{(2\pi)^2}\int \frac{d^2\underline{k}}{\underline{k}^2}\, \Phi^{up}(\underline{k},\, \underline{r}-\underline{k}) \int \frac{d^2\underline{k}'}{\underline{k}'^2}\, \Phi^{down}(-\underline{k}',\, -\underline{r}+\underline{k}') \times \int_{\delta-i\infty}^{\delta+i\infty} \frac{d\omega}{2\pi i} \left(\frac{s}{s_0}\right)^{\omega} G_\omega(\underline{k}, \underline{k}', \underline{r})$$

$\longleftarrow$ multi-Regge kinematics

$\Rightarrow$ set $\beta_n = 0$ and $\int d\alpha_n$ $\Rightarrow$ $\Phi^{\gamma^*\to\gamma^*}(-\underline{k}_n, -\underline{r} + \underline{k}_n)$

Mueller Navelet jets at LL BFKL

- in LL BFKL ($\sim \sum (\alpha_s \ln s)^n$), emission between these jets $\longrightarrow$ strong decorrelation between the relative azimuthal angle jets, incompatible with $p\bar{p}$ Tevatron collider data
- a collinear treatment at next-to-leading order (NLO) can describe the data
- important issue: non-conservation of energy-momentum along the BFKL ladder. A LL BFKL-based Monte Carlo combined with e-m conservation improves dramatically the situation (Orr and Stirling)

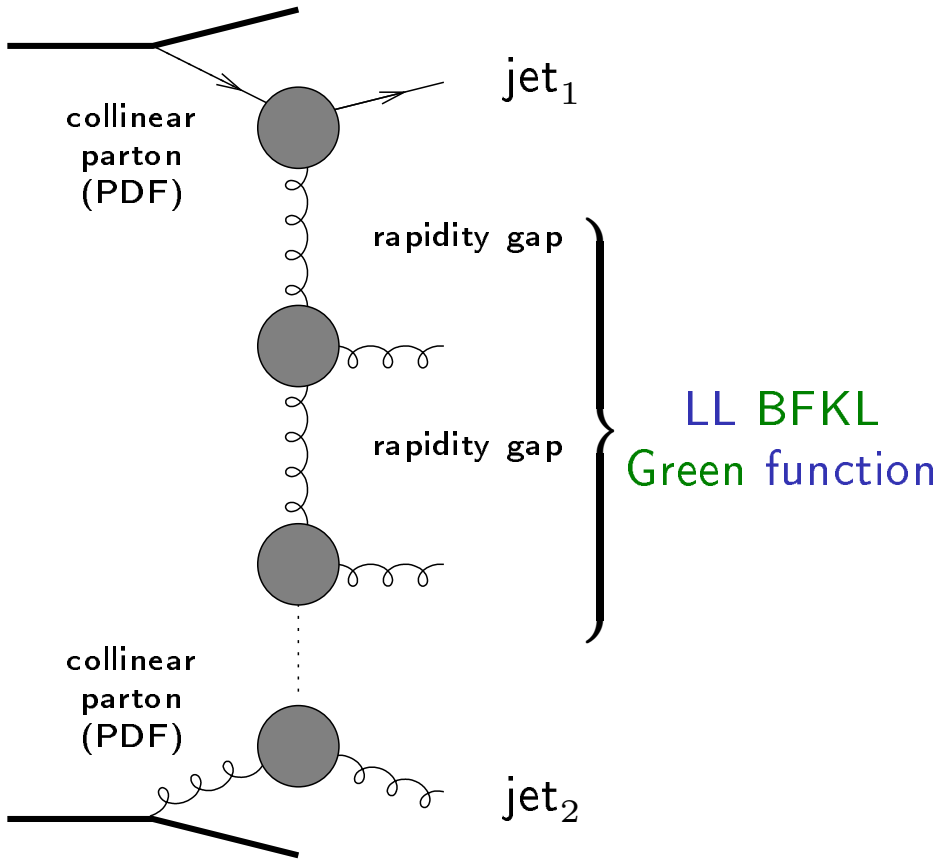

Multi-Regge kinematics (LL BFKL)

Mueller Navelet jets at NLL BFKL

- up to now, the subseries $\alpha_s \sum (\alpha_s \ln s)^n$ NLL was included only in the exchanged $\mathbb{P}$omeron state, and not inside the jet vertices
  Sabio Vera, Schwennsen
  Marquet, Royon
- the common belief was that these corrections should not be important

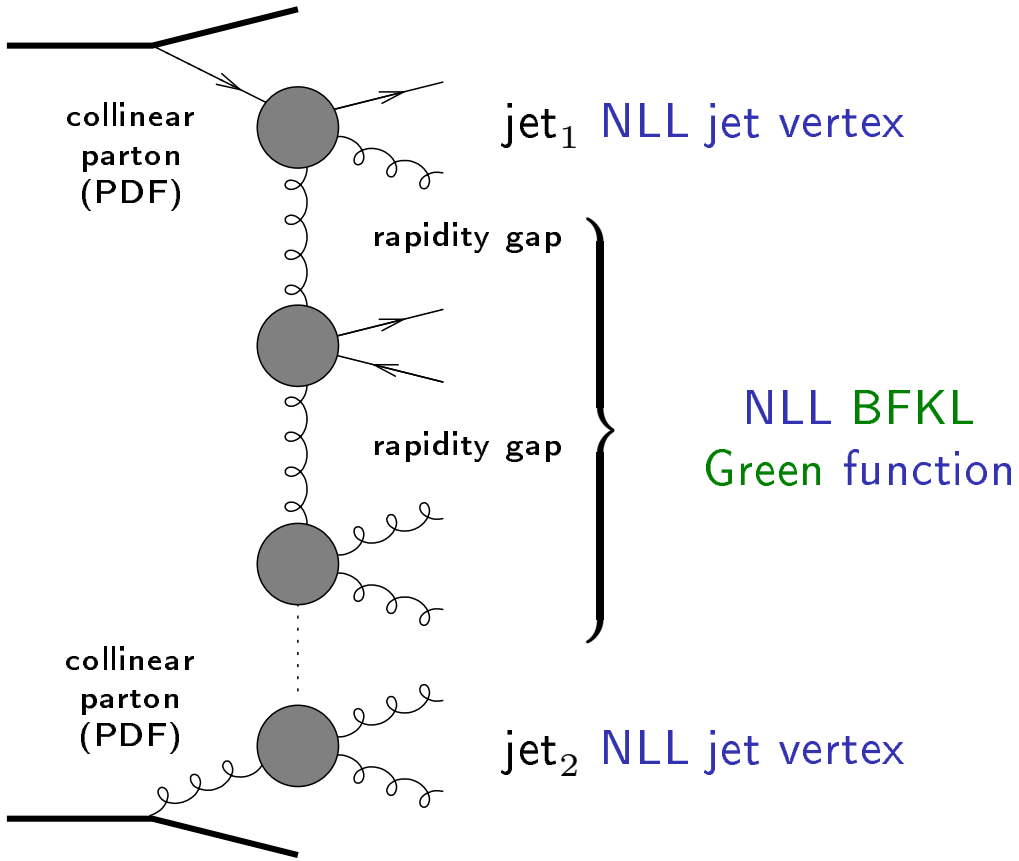

Quasi Multi-Regge kinematics (here for NLL BFKL)

Angular coefficients

$$\mathcal{C}_m \equiv \int \mathrm{d}\phi_{J1}\,\mathrm{d}\phi_{J2}\,\cos\left(m(\phi_{J,1}-\phi_{J,2}-\pi)\right)$$
$$\times \int \mathrm{d}^2\mathbf{k}_1\,\mathrm{d}^2\mathbf{k}_2\,\Phi(\mathbf{k}_{J1},x_{J,1},-\mathbf{k}_1)\,G(\mathbf{k}_1,\mathbf{k}_2,\hat{s})\,\Phi(\mathbf{k}_{J2},x_{J,2},\mathbf{k}_2).$$

- $m=0 \implies$ cross-section

$$\frac{\mathrm{d}\sigma}{\mathrm{d}|\mathbf{k}_{J1}|\,\mathrm{d}|\mathbf{k}_{J2}|\,\mathrm{d}y_{J1}\,\mathrm{d}y_{J2}} = \mathcal{C}_0$$

- $m>0 \implies$ azimuthal decorrelation

$$\langle\cos(m\phi)\rangle \equiv \langle\cos\left(m(\phi_{J,1}-\phi_{J,2}-\pi)\right)\rangle = \frac{\mathcal{C}_m}{\mathcal{C}_0}$$

Rely on LL BFKL eigenfunctions

- LL BFKL eigenfunctions:
  $E_{n,\nu}(\mathbf{k}_1) = \frac{1}{\pi\sqrt{2}} \left(\mathbf{k}_1^2\right)^{i\nu-\frac{1}{2}} e^{in\phi_1}$
- decompose Φ on this basis
- use the known LL eigenvalue of the BFKL equation on this basis:

$$\omega(n,\nu) = \bar{\alpha}_s \chi_0\left(|n|, \tfrac{1}{2} + i\nu\right)$$

with $\chi_0(n,\gamma) = 2\Psi(1) - \Psi\left(\gamma + \frac{n}{2}\right) - \Psi\left(1 - \gamma + \frac{n}{2}\right)$

$(\Psi(x) = \Gamma'(x)/\Gamma(x),\ \bar{\alpha}_s = N_c \alpha_s/\pi)$

- $\Longrightarrow$ master formula:

$$\mathcal{C}_m = (4 - 3\,\delta_{m,0}) \int \mathrm{d}\nu\, C_{m,\nu}(|\mathbf{k}_{J1}|, x_{J,1})\, C^*_{m,\nu}(|\mathbf{k}_{J2}|, x_{J,2}) \left(\frac{\hat{s}}{s_0}\right)^{\omega(m,\nu)}$$

with $$C_{m,\nu}(|\mathbf{k}_J|, x_J) = \int \mathrm{d}\phi_J\, \mathrm{d}^2\mathbf{k}\, \mathrm{d}x\, f(x) V(\mathbf{k}, x) E_{m,\nu}(\mathbf{k}) \cos(m\phi_J)$$

- at NLL, same master formula: just change $\omega(m,\nu)$ and V
  (although $E_{n,\nu}$ are not anymore eigenfunctions)

NLL Green's function: rely on LL BFKL eigenfunctions

- NLL BFKL kernel is not conformal invariant
- LL $E_{n,\nu}$ are not anymore eigenfunction
- this can be overcome by considering the eigenvalue as an operator with a part containing $\frac{\partial}{\partial \nu}$
- it acts on the impact factor

$$\omega(n,\nu) = \bar{\alpha}_s \chi_0\left(|n|, \frac{1}{2}+i\nu\right) + \bar{\alpha}_s^2 \left[\chi_1\left(|n|, \frac{1}{2}+i\nu\right) - \frac{\pi b_0}{2N_c}\chi_0\left(|n|, \frac{1}{2}+i\nu\right) \underbrace{\left\{-2\ln\mu_R^2 - i\frac{\partial}{\partial\nu}\ln\frac{C_{n,\nu}(|\mathbf{k}_{J1}|, x_{J,1})}{C_{n,\nu}(|\mathbf{k}_{J2}|, x_{J,2})}\right\}}_{2\ln\frac{|\mathbf{k}_{J1}|\cdot|\mathbf{k}_{J2}|}{\mu_R^2}}\right],$$

Collinear improved Green's function at NLL

- one may improve the NLL BFKL kernel for $n = 0$ by imposing its compatibility with DGLAP in the collinear limit
  Salam; Ciafaloni, Colferai
- usual (anti)collinear poles in $\gamma = 1/2 + i\nu$ (resp. $1 - \gamma$) are shifted by $\omega/2$
- one practical implementation:
  - the new kernel $\bar{\alpha}_s \chi^{(1)}(\gamma, \omega)$ with shifted poles replaces

    $$\bar{\alpha}_s \chi_0(\gamma, 0) + \bar{\alpha}_s^2 \chi_1(\gamma, 0)$$

  - $\omega(0, \nu)$ is obtained by solving the implicit equation

    $$\omega(0, \nu) = \bar{\alpha}_s \chi^{(1)}(\gamma, \omega(0, \nu))$$

    for $\omega(n, \nu)$ numerically.
- there is no need for any jet vertex improvement because of the absence of γ and $1 - \gamma$ poles (numerical proof using Cauchy theorem "backward")

Jet vertex: LL versus NLL

$\mathbf{k}, \mathbf{k}'$ = Euclidian two dimensional vectors

LL jet vertex:

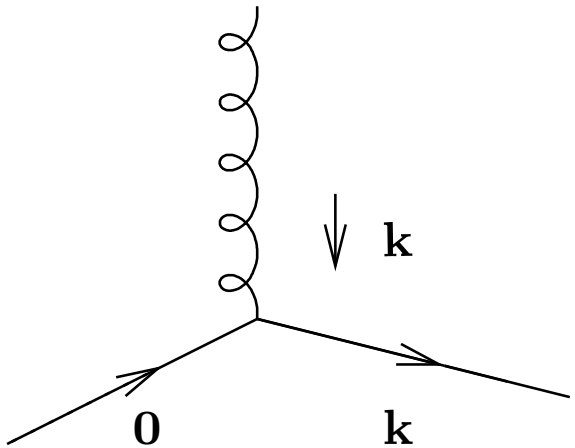

NLL jet vertex:

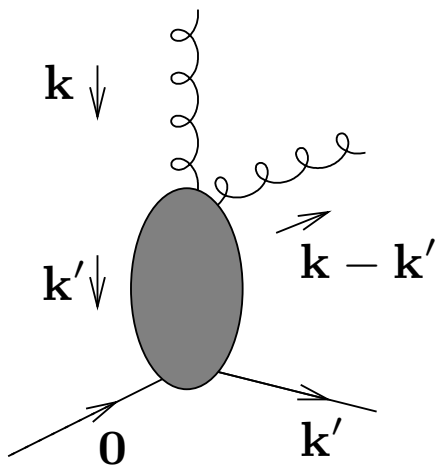

$$V_{\rm a}^{(0)}(\mathbf{k},x) = h_{\rm a}^{(0)}(\mathbf{k})\mathcal{S}_J^{(2)}(\mathbf{k};x)$$

with: $$h_{\rm a}^{(0)}(\mathbf{k}) = \frac{\alpha_s}{\sqrt{2}}\frac{C_{A/F}}{\mathbf{k}^2}\,,$$

$$\mathcal{S}_J^{(2)}(\mathbf{k};x) = \delta\left(1-\frac{x_J}{x}\right)|\mathbf{k}_J|\delta^{(2)}(\mathbf{k}-\mathbf{k}_J)$$

NLL corrections to the jet vertex: the quark part (Bartels, Colferai, Vacca)

$$
\begin{aligned}
V_{\mathrm{q}}^{(1)}(\mathbf{k},x) = &\left[\left(\frac{3}{2}\ln\frac{\mathbf{k}^2}{\Lambda^2}-\frac{15}{4}\right)\frac{C_F}{\pi}+\left(\frac{85}{36}+\frac{\pi^2}{4}\right)\frac{C_A}{\pi}-\frac{5}{18}\frac{N_f}{\pi}-b_0\ln\frac{\mathbf{k}^2}{\mu^2}\right]V_{\mathrm{q}}^{(0)}(\mathbf{k},x)\\
&+\int \mathrm{d}z\left(\frac{C_F}{\pi}\frac{1-z}{2}+\frac{C_A}{\pi}\frac{z}{2}\right)V_{\mathrm{q}}^{(0)}(\mathbf{k},xz)\\
&+\frac{C_A}{\pi}\int\frac{\mathrm{d}^2\mathbf{k}'}{\pi}\int\mathrm{d}z\left[\frac{1+(1-z)^2}{2z}\left((1-z)\frac{(\mathbf{k}-\mathbf{k}')\cdot((1-z)\mathbf{k}-\mathbf{k}')}{(\mathbf{k}-\mathbf{k}')^2((1-z)\mathbf{k}-\mathbf{k}')^2}h_{\mathrm{q}}^{(0)}(\mathbf{k}')\mathcal{S}_J^{(3)}(\mathbf{k}',\mathbf{k}-\mathbf{k}',xz;x)\right.\right.\\
&\qquad\left.-\frac{1}{\mathbf{k}'^2}\Theta(\Lambda^2-\mathbf{k}'^2)V_{\mathrm{q}}^{(0)}(\mathbf{k},xz)\right)\\
&\qquad\left.-\frac{1}{z(\mathbf{k}-\mathbf{k}')^2}\Theta(|\mathbf{k}-\mathbf{k}'|-z(|\mathbf{k}-\mathbf{k}'|+|\mathbf{k}'|))V_{\mathrm{q}}^{(0)}(\mathbf{k}',x)\right]\\
&+\frac{C_F}{2\pi}\int\mathrm{d}z\,\frac{1+z^2}{1-z}\int\frac{\mathrm{d}^2\mathbf{l}}{\pi\mathbf{l}^2}\left[\frac{\mathcal{N}C_F}{\mathbf{l}^2+(\mathbf{l}-\mathbf{k})^2}\left(\mathcal{S}_J^{(3)}(z\mathbf{k}+(1-z)\mathbf{l},(1-z)(\mathbf{k}-\mathbf{l}),x(1-z);x)\right.\right.\\
&\qquad\left.+\mathcal{S}_J^{(3)}(\mathbf{k}-(1-z)\mathbf{l},(1-z)\mathbf{l},x(1-z);x)\right)\\
&\qquad\left.-\Theta\left(\frac{\Lambda^2}{(1-z)^2}-\mathbf{l}^2\right)\left(V_{\mathrm{q}}^{(0)}(\mathbf{k},x)+V_{\mathrm{q}}^{(0)}(\mathbf{k},xz)\right)\right]\\
&-\frac{2C_F}{\pi}\int\mathrm{d}z\left(\frac{1}{1-z}\right)\int\frac{\mathrm{d}^2\mathbf{l}}{\pi\mathbf{l}^2}\left[\frac{\mathcal{N}C_F}{\mathbf{l}^2+(\mathbf{l}-\mathbf{k})^2}S_J^{(2)}(\mathbf{k},x)-\Theta\left(\frac{\Lambda^2}{(1-z)^2}-\mathbf{l}^2\right)V_{\mathrm{q}}^{(0)}(\mathbf{k},x)\right]
\end{aligned}
$$

NLL corrections to the jet vertex: the gluon part (Bartels, Colferai, Vacca)

$$
\begin{aligned}
V_{\mathrm{g}}^{(1)}(\mathbf{k},x) = {} & \left[\left(\frac{11}{6}\frac{C_A}{\pi}-\frac{1}{3}\frac{N_f}{\pi}\right)\ln\frac{\mathbf{k}^2}{\Lambda^2}+\left(\frac{\pi^2}{4}-\frac{67}{36}\right)\frac{C_A}{\pi}+\frac{13}{36}\frac{N_f}{\pi}-b_0\ln\frac{\mathbf{k}^2}{\mu^2}\right]V_{\mathrm{g}}^{(0)}(\mathbf{k},x) \\
& + \int \mathrm{d}z\,\frac{N_f}{\pi}\frac{C_F}{C_A}z(1-z)V_{\mathrm{g}}^{(0)}(\mathbf{k},xz) \\
& + \frac{N_f}{\pi}\int\frac{\mathrm{d}^2\mathbf{k}'}{\pi}\int_0^1 \mathrm{d}z\,P_{\mathrm{qg}}(z)\left[\frac{h_{\mathrm{q}}^{(0)}(\mathbf{k}')}{(\mathbf{k}-\mathbf{k}')^2+\mathbf{k}'^2}\mathcal{S}_J^{(3)}(\mathbf{k}',\mathbf{k}-\mathbf{k}',xz;x)-\frac{1}{\mathbf{k}'^2}\Theta(\Lambda^2-\mathbf{k}'^2)V_{\mathrm{q}}^{(0)}(\mathbf{k},xz)\right] \\
& + \frac{N_f}{2\pi}\int\frac{\mathrm{d}^2\mathbf{k}'}{\pi}\int_0^1 \mathrm{d}z\,P_{\mathrm{qg}}(z)\frac{\mathcal{N}C_A}{((1-z)\mathbf{k}-\mathbf{k}')^2}\left[z(1-z)\frac{(\mathbf{k}-\mathbf{k}')\cdot\mathbf{k}'}{(\mathbf{k}-\mathbf{k}')^2\mathbf{k}'^2}\mathcal{S}_J^{(3)}(\mathbf{k}',\mathbf{k}-\mathbf{k}',xz;x)\right. \\
& \qquad \left. -\frac{1}{\mathbf{k}^2}\Theta\left(\Lambda^2-((1-z)\mathbf{k}-\mathbf{k}')^2\right)\mathcal{S}_J^{(2)}(\mathbf{k},x)\right] \\
& + \frac{C_A}{\pi}\int_0^1\frac{\mathrm{d}z}{1-z}\left[(1-z)P(1-z)\right]\int\frac{\mathrm{d}^2\mathbf{l}}{\pi\mathbf{l}^2}\left\{\frac{\mathcal{N}C_A}{\mathbf{l}^2+(\mathbf{l}-\mathbf{k})^2}\left[\mathcal{S}_J^{(3)}(z\mathbf{k}+(1-z)\mathbf{l},(1-z)(\mathbf{k}-\mathbf{l}),x(1-z);x)\right.\right. \\
& \qquad \left. + \mathcal{S}_J^{(3)}(\mathbf{k}-(1-z)\mathbf{l},(1-z)\mathbf{l},x(1-z);x)\right] \\
& \qquad \left. -\Theta\left(\frac{\Lambda^2}{(1-z)^2}-\mathbf{l}^2\right)\left[V_{\mathrm{g}}^{(0)}(\mathbf{k},x)+V_{\mathrm{g}}^{(0)}(\mathbf{k},xz)\right]\right\} \\
& - \frac{2C_A}{\pi}\int_0^1\frac{\mathrm{d}z}{1-z}\int\frac{\mathrm{d}^2\mathbf{l}}{\pi\mathbf{l}^2}\left[\frac{\mathcal{N}C_A}{\mathbf{l}^2+(\mathbf{l}-\mathbf{k})^2}S_J^{(2)}(\mathbf{k},x)-\Theta\left(\frac{\Lambda^2}{(1-z)^2}-\mathbf{l}^2\right)V_{\mathrm{g}}^{(0)}(\mathbf{k},x)\right] \\
& + \frac{C_A}{\pi}\int\frac{\mathrm{d}^2\mathbf{k}'}{\pi}\int_0^1\mathrm{d}z\left[P(z)\left((1-z)\frac{(\mathbf{k}-\mathbf{k}')\cdot((1-z)\mathbf{k}-\mathbf{k}')}{(\mathbf{k}-\mathbf{k}')^2((1-z)\mathbf{k}-\mathbf{k}')^2}h_{\mathrm{g}}^{(0)}(\mathbf{k}')\right.\right. \\
& \qquad \left.\times\mathcal{S}_J^{(3)}(\mathbf{k}',\mathbf{k}-\mathbf{k}',xz;x)-\frac{1}{\mathbf{k}'^2}\Theta(\Lambda^2-\mathbf{k}'^2)V_{\mathrm{g}}^{(0)}(\mathbf{k},xz)\right) \\
& \qquad \left.-\frac{1}{z(\mathbf{k}-\mathbf{k}')^2}\Theta(|\mathbf{k}-\mathbf{k}'|-z(|\mathbf{k}-\mathbf{k}'|+|\mathbf{k}'|))V_{\mathrm{g}}^{(0)}(\mathbf{k}',x)\right]
\end{aligned}
$$

Jet algorithms

- a jet algorithm should be IR safe, both for soft and collinear singularities
- the most common jet algorithm are:
  - k_t algorithms (IR safe but time consuming for multiple jets configurations)
  - cone algorithm (not IR safe in general; can be made IR safe at NLO: Ellis, Kunszt, Soper)

Cone jet algorithm at NLO (Ellis, Kunszt, Soper)

- Should partons $(|\mathbf{p}_1|, \phi_1, y_1)$ and $(\mathbf{p}_2|, \phi_2, y_2)$ be combined in a single jet?
  $|\mathbf{p}_i|$ =transverse energy deposit in the calorimeter cell i of parameter $\Omega = (y_i, \phi_i)$ in $y - \phi$ plane
- define transverse energy of the jet: $p_J = |\mathbf{p}_1| + |\mathbf{p}_2|$
- jet axis:

$$\Omega_c \begin{cases} y_J = \dfrac{|\mathbf{p}_1|\, y_1 + |\mathbf{p}_2|\, y_2}{p_J} \\ \phi_J = \dfrac{|\mathbf{p}_1|\, \phi_1 + |\mathbf{p}_2|\, \phi_2}{p_J} \end{cases}$$

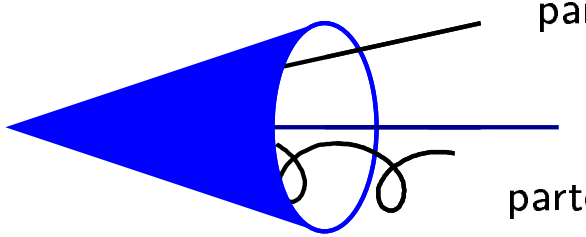

$\Omega = (y_i, \phi_i)$ in $y - \phi$ plane

If distances $|\Omega_i - \Omega_c|^2 \equiv (y_i - y_c)^2 + (\phi_i - \phi_c)^2 < R^2$ $(i = 1$ and $i = 2)$

$\Longrightarrow$ partons 1 and 2 are in the same cone Ω_c

combined condition: $|\Omega_1 - \Omega_2| < \dfrac{|\mathbf{p}_1| + |\mathbf{p}_2|}{max(|\mathbf{p}_1|, |\mathbf{p}_2|)} R$

LL jet vertex and cone algorithm

$\mathbf{k}, \mathbf{k}'$ = Euclidian two dimensional vectors

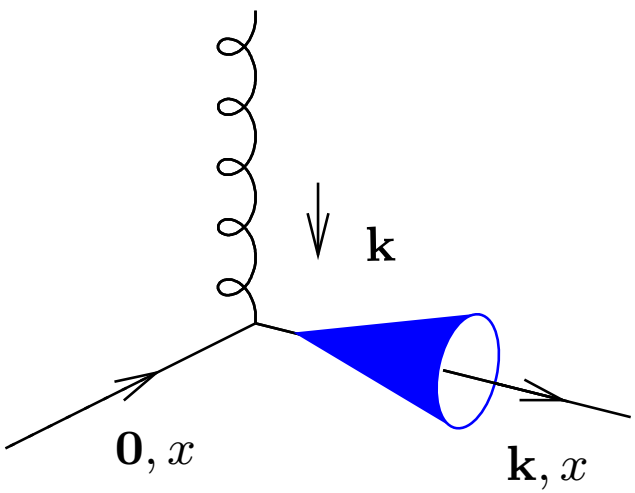

$$\mathcal{S}_J^{(2)}(k_\perp; x) = \delta\left(1 - \frac{x_J}{x}\right) |\mathbf{k}|\, \delta^{(2)}(\mathbf{k} - \mathbf{k}_J)$$

NLL jet vertex and cone algorithm

$\mathbf{k}, \mathbf{k}'$ = Euclidian two dimensional vectors

$$\mathcal{S}_J^{(3,\text{cone})}(\mathbf{k}', \mathbf{k}-\mathbf{k}', xz; x) =$$

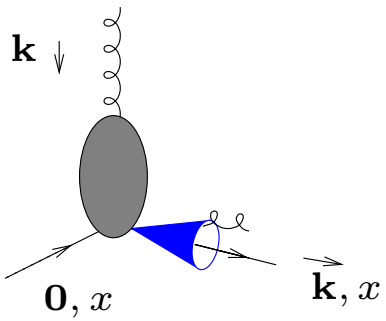

$$\mathcal{S}_J^{(2)}(\mathbf{k}, x)\,\Theta\left(\left[\frac{|\mathbf{k}-\mathbf{k}'|+|\mathbf{k}'|}{\max(|\mathbf{k}-\mathbf{k}'|,|\mathbf{k}'|)}R_{\text{cone}}\right]^2 - \left[\Delta y^2+\Delta\phi^2\right]\right)$$

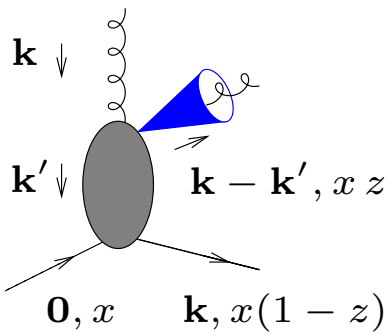

$$+\,\mathcal{S}_J^{(2)}(\mathbf{k}-\mathbf{k}', xz)\,\Theta\left(\left[\Delta y^2+\Delta\phi^2\right] - \left[\frac{|\mathbf{k}-\mathbf{k}'|+|\mathbf{k}'|}{\max(|\mathbf{k}-\mathbf{k}'|,|\mathbf{k}'|)}R_{\text{cone}}\right]^2\right)$$

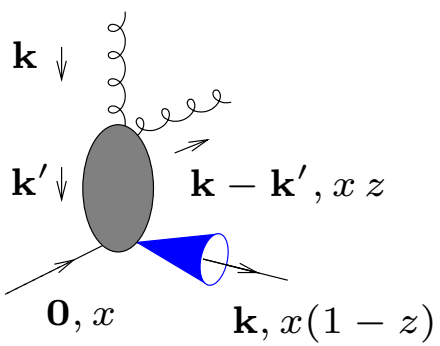

$$+\,\mathcal{S}_J^{(2)}(\mathbf{k}', x(1-z))\,\Theta\left(\left[\Delta y^2+\Delta\phi^2\right] - \left[\frac{|\mathbf{k}-\mathbf{k}'|+|\mathbf{k}'|}{\max(|\mathbf{k}-\mathbf{k}'|,|\mathbf{k}'|)}R_{\text{cone}}\right]^2\right),$$

Mueller-Navelet jets at NLL and finiteness

Using a IR safe jet algorithm, Mueller-Navelet jets at NLL are finite

- UV sector:
  - the NLL impact factor contains UV divergencies $1/\epsilon$
  - they are absorbed by the renormalization of the coupling: $\alpha_S \longrightarrow \alpha_S(\mu_R)$
- IR sector:
  - PDF have IR collinear singularities: pole $1/\epsilon$ at LO
  - these collinear singularities can be compensated by collinear singularities of the two jets vertices and the real part of the BFKL kernel
  - the remaining collinear singularities compensate exactly among themselves
  - soft singularities of the real and virtual BFKL kernel, and of the jets vertices compensates among themselves

This was shown for both quark and gluon initiated vertices (Bartels, Colferai, Vacca)

LL substraction and s_0

- one sums up $\sum(\alpha_s \ln \hat{s}/s_0)^n + \alpha_s \sum(\alpha_s \ln \hat{s}/s_0)^n \quad (\hat{s} = x_1\, x_2\, s)$
- at LL s_0 is arbitrary

- natural choice: $s_0 = \sqrt{s_{0,1}\, s_{0,2}}$ $s_{0,i}$ for each of the scattering objects
  - possible choice: $s_{0,i} = (|\mathbf{k}_J| + |\mathbf{k}_J - \mathbf{k}|)^2$ (Bartels, Colferai, Vacca)
    - but depend on $\mathbf{k}$, which is integrated over
    - $\hat{s}$ is not an external scale ($x_{1,2}$ are integrated over)
  - we prefer

$$\left.\begin{aligned} s_{0,1} = (|\mathbf{k}_{J1}| + |\mathbf{k}_{J1} - \mathbf{k}_1|)^2 \;\to\; s'_{0,1} = \frac{x_1^2}{x_{J,1}^2}\mathbf{k}_{J1}^2 \\ s_{0,2} = (|\mathbf{k}_{J2}| + |\mathbf{k}_{J2} - \mathbf{k}_2|)^2 \;\to\; s'_{0,2} = \frac{x_2^2}{x_{J,2}^2}\mathbf{k}_{J2}^2 \end{aligned}\right\} \quad \frac{\hat{s}}{s_0} \;\to\; \frac{\hat{s}}{s'_0} = \frac{x_{J,1}\, x_{J_2}\, s}{|\mathbf{k}_{J1}|\,|\mathbf{k}_{J2}|} = e^{y_{J,1} - y_{J,2}} \equiv e^Y$$

- $s_0 \to s'_0$ affects
  - the BFKL NLL Green function
  - the impact factors:

$$\Phi_{\rm NLL}(\mathbf{k}_i; s'_{0,i}) = \Phi_{\rm NLL}(\mathbf{k}_i; s_{0,i}) + \int \mathrm{d}^2\mathbf{k}'\, \Phi_{\rm LL}(\mathbf{k}'_i)\, \mathcal{K}_{\rm LL}(\mathbf{k}'_i, \mathbf{k}_i) \frac{1}{2} \ln \frac{s'_{0,i}}{s_{0,i}} \qquad (1)$$

- numerical stability (non azimuthal averaging of LL substraction) improved with the choice $s_{0,i} = (\mathbf{k}_i - 2\mathbf{k}_{Ji})^2$
  (then replaced by $s'_{0,i}$ after numerical integration)
- (1) can be used to test $s_0 \to \lambda\, s_0$ dependence

Motivation for asymmetric configurations

- Initial state radiation (unseen) produces divergencies if one touches the collinear singularity $\mathbf{q}^2 \to 0$

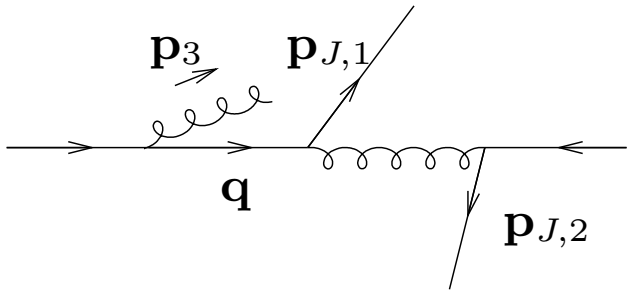

- they are compensated by virtual corrections
- this compensation is in practice difficult to implement when for some reason this additional emission is in a "corner" of the phase space (dip in the differential cross-section)
- this is the case when $\mathbf{p}_1 + \mathbf{p}_2 \to 0$
- this calls for a resummation of large remaing logs $\Rightarrow$ Sudakov resummation

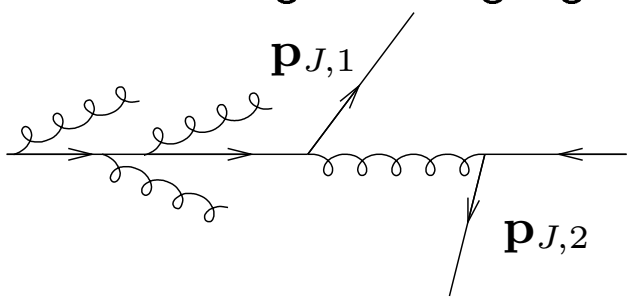

Motivation for asymmetric configurations

- since these resummation have never been investigated in this context, one should better avoid that region
- note that for BFKL, due to additional emission between the two jets, one may expect a less severe problem (at least a smearing in the dip region $|\mathbf{p}_1| \sim |\mathbf{p}_2|$)

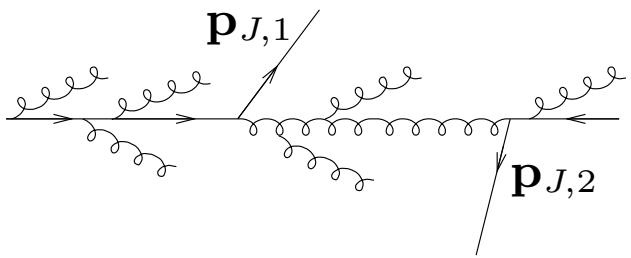

- this may however not mean that the region $|\mathbf{p}_1| \sim |\mathbf{p}_2|$ is perfectly trustable even in a BFKL type of treatment
- we now investigate a region where NLL DGLAP is under control